Insights into ROS-dependent signalling underlying transcriptomic plant responses to the herbicide 2,4-D

María C. Romero-Puertas[1]*, M. Ángeles Peláez-Vico[1], Diana M. Pazmiño[1], María Rodríguez-Serrano[1#], Rocío Bautista[2], Aurelio Gómez-Cadenas[3], M. Gonzalo Claros[2,4,5], José León[6], Luisa M. Sandalio[1]*

[1]*Departamento de Bioquímica, Biología Celular y Molecular de Plantas, EEZ, CSIC, C/ Prof. Albareda, 18008 Granada, Spain*
[2]*Plataforma Andaluza de Bioinformática-SCBI, Universidad de Málaga, C/Severo Ochoa 34, 29590 Málaga, Spain*
[3]*Department Ciències Agràries i del Medi Natural, Universitat Jaume I, E-12071, Castelló de la Plana, Spain*
[4]*Departamento de Biología Molecular y Bioquímica, Ciencias, Univ. de Málaga, Campus de Teatinos s/n, 29071, Málaga, Spain*
[5]*Institute for Mediterranean and Subtropical Horticulture "La Mayora" (IHSM-UMA-CSIC), Av. Louis Pasteur, 49. 29010 Málaga, Spain*
[6]*Instituto de Biología Molecular y Celular de Plantas (CSIC-Univ. Valencia), CPI Edificio 8E, Avda. Ingeniero Fausto Elio s/n, 46022 Valencia, Spain*

[#]*Current address: Education Faculty, University of Granada, Melilla, Spain*

*Authors for correspondence:

Dr. Luisa M. Sandalio

Telephone: +34958181600 Ext. 316

e-mail: luisamaria.sandalio@eez.csic.es

Dr. María C. Romero-Puertas

Telephone: +34958181600 Ext. 175

e-mail: maria.romero@eez.csic.es

Key words: 2,4-D; Acyl-CoA oxidase; auxin; peroxisomes; reactive oxygen species; signalling; transcriptome

ABSTRACT

The synthetic auxin 2,4-dichlorophenoxyacetic acid (2,4-D) functions as an agronomic weed control herbicide. High concentrations of 2,4-D induce plant growth defects, particularly leaf epinasty and stem curvature. Although the 2,4-D phenotype is associated with ROS production, little is known about ROS-dependent signalling. In this study, by using T-DNA Arabidopsis mutants to silence peroxisomal acyl CoA oxidase 1 (*acx1-2*), we identified ACX1 as one of the main sources of ROS production and as partly the cause of the epinasty phenotype following the application of 2,4-D. Transcriptomic analyses of WT plants after treatment with 2,4-D revealed a ROS-related peroxisomal footprint in early plant responses, while other organelles, such as mitochondria and chloroplasts, are involved in later responses. Interestingly, a group of ACX1-dependent transcripts in plant responses to 2,4-D, previously associated with epinasty, is related to auxin biosynthesis, metabolism and signalling. We found that protein AUXIN SIGNALING F-BOX 3 (AFB3), a component of SCF (ASK-cullin-F-box) E3 ubiquitin ligase complexes, which functions as an auxin receptor and mediates Aux/IAA proteasomal degradation, acts downstream of ACX1 and is involved in the epinasty phenotype induced by 2,4-D. We also found that protein degradation associated with ubiquitin E3-RING and E3-SCF-FBOX in ACX1-dependent signalling in plant responses to 2,4-D is significantly regulated over longer treatment periods.

INTRODUCTION

2,4-Dichlorophenoxyacetic acid (2,4-D) is one of the most commonly used auxinic herbicides in agriculture (Burns and Swaen, 2012). In fact, new 2,4-D-resistant crops have been approved by the U.S. Department of Agriculture in the previous ten years (Egan *et al.*, 2011), suggesting current contamination of soil and water that can affect the environment and even human health (Teixeira *et al.*, 2007; Zuanazzi *et al.*, 2020; Li *et al.*, 2021). Given that 2,4-D is a synthetic andanalogue of natural auxins, low concentrations of indole-3-acetic acid (IAA) have been found to stimulate plant growth (Enders and Strader, 2015). At higher concentrations however, 2,4-D induces plant growth defects, particularly stem curvature, leaf epinasty, senescence and root growth inhibition (Grossmann *et al.*, 2001; Romero-Puertas *et al.*, 2004a; Pazmiño *et al.,* 2012).

Auxin modulates the expression of genes regulated by the interplay of auxin response factors (ARFs) and auxin/indole acetic acid (Aux/IAA) repressors. At low auxin concentrations, Aux/IAA repress ARF activators and block auxin-regulated gene expression; however, higher concentrations of auxin promote the binding of auxin to Transport Inhibitor Response1/Auxin Signalling F-Box (TIR1/AFB) receptors; this leads to degradation of Aux/IAA repressors by the 26S proteasome, which promotes auxin-dependent gene expression (Eyer *et al.*, 2016; Sandalio *et al.*, 2016). 2,4-D has been reported to be a poor substrate for the auxin receptor ABP1 (Gao *et al.*, 2015), and probably acts via TIR1/AFB auxin-mediated signalling (Parry *et al.*, 2009; Eyer *et al.*, 2016). The TIR1/AFB gene family consists of six receptors: TIR1 and five AFB homologs (Prigge *et al.*, 2016). Analysis of Arabidopsis mutant lines of TIR and AFB has demonstrated that these receptors are indeed essential for the plant perception and specificity of auxin herbicides (McCauley *et al.*, 2020).

A close relationship between reactive oxygen species (ROS) has been established in both auxin-dependent cell growth and 2,4-D mode of action. Thus, hydroxyl radicals (·OH) are involved in the cleavage of covalent bonds in the cell wall during plant growth (Liszkay *et al.*, 2004), and ROS have been shown to affect auxin homeostasis and conjugation, with the degradation, distribution and relocation of IAA giving rise to morphological changes (reviewed in Sandalio *et al.*, 2016). ROS over-accumulation and oxidative stress are two of the main effects of the herbicide 2,4-D which increases lipid and protein

oxidation and induces proteolysis (Romero-Puertas *et al.*, 2004a; Pazmiño *et al.*, 2011, 2012). 2,4-D has been shown to affect actin cytoskeleton structures, probably due to the *S*-nitrosylation and carbonylation of actin; these post-translational modifications (PTMs) disrupt actin polymerization and cytoskeleton structures, leading to increased epinasty and alterations in the dynamics of organelles such as peroxisomes and mitochondria (Rodríguez-Serrano *et al.*, 2014). The dysfunction of these organelles may contribute to the accumulation of ROS, as was observed following treatment of pea and Arabidopsis plants with 2,4-D (Romero-Puertas *et al.*, 2004a; Pazmiño *et al.*, 2011; Rodríguez-Serrano *et al.*, 2014). The peroxisomal enzymes xanthine oxidase (XOD) and acyl-CoA oxidase (ACX) have been suggested as possible sources of ROS following 2,4-D treatment (Romero-Puertas *et al.*, 2004a; Pazmiño *et al.*, 2011, 2014), indicating that peroxisomes are key organelles in plant responses to this herbicide. Peroxisomes, which can produce and remove ROS efficiently, have the capacity to regulate oxidative metabolism (Sandalio and Romero-Puertas, 2015; Sandalio *et al.,* 2021). Peroxisomes, whose metabolism and dynamic peroxisomal plasticity enable changes to be made in their enzymatic composition, size, shape, number and motility under different situations, play a key decision-making role in the cell (Kao *et al.*, 2018; Sandalio *et al.,* 2021).

Fatty acid β-oxidation is one of the main sources of ROS, particularly H_2O_2, in peroxisomes (Pan *et al.*, 2020). ACX, the first enzyme in the pathway, catalyzes the oxidation of acyl-CoA to trans-2-enoyl-CoA, leading to the production of H_2O_2 in the reaction (Rinaldi *et al.*, 2016). This pathway, which provides energy from fats stored in oil bodies, is highly active at the initial stage of seedling growth (Rinaldi *et al.*, 2016). β-oxidation, which is involved in the synthesis of key metabolites, including hormones such as indole acetic acid (IAA) and jasmonic acid (JA), also occurs in green tissues (Pan *et al.*, 2020; Sandalio *et al.,* 2021).

Although 2,4-D-dependent oxidative effects in plants have been widely characterized, little is known about their underlying signaling mechanisms and the role of ROS in regulating plant responses to 2,4-D. In this study, we observed a decrease in H_2O_2 associated with *β*-oxidation in response to the herbicide 2,4-D. By analyzing transcriptomic responses in Arabidopsis plants, WT and the mutant *acx1-2*, with a T-DNA insertion in *ACX1*, our results suggest that H_2O_2 produced

during *β*-oxidation regulates several sets of early genes related to IAA homeostasis, transport and signalling, leading to regulation of leaf epinasty. Longer exposure to 2,4-D involved other organelles such as mitochondria and chloroplast in regulating ROS-dependent contributions to 2,4-D activity.

MATERIALS AND METHODS

Plant Material and 2,4-D treatment

Col-0 was the background used for all the Arabidopsis seeds in the study: WT and the transgenic lines *acx1-2* (kindly donated by Dr. J. León; SALK_041464), *acx1-4* and *afb3-1* (from the Nottingham Arabidopsis Stock Centre, NASC). Seeds were sown in moistened soil and grown in 16 h light and 8 h dark photoperiod cycles at 22 and 20 ºC, respectively, under 120 µE and at 60 % relative humidity. Genomic DNA PCR analysis of *acx1-4* (SALK_145527) and *afb3-1* (SALK_068787C) lines was carried out to verify homozygosity in T-DNA insertions with the appropriate primers (Suppl. Table S1; Suppl. Fig. S1 A-B; Fig. 6), while *acx1-2* has been characterized elsewhere (Adham et al., 2005). The effect of 2,4-dichlorophenoxyacetic acid (2,4-D) on Arabidopsis plants was analysed by spraying 23 mM 2,4-D solution (1% dimethyl sulfoxide acid, DMSO and 1% EtOH), and plant leaves were collected after 1 and 72 h post treatment (hpt). Control plants were sprayed with 1% DMSO and 1% EtOH. Treatment times, 2,4-D concentrations and treatment techniques used in this study had been previously optimised (Romero-Puertas et al., 2004a; Pazmiño et al., 2014; Rodríguez-Serrano et al., 2014).

H_2O_2 quantification and localization

Hydrogen peroxide (H_2O_2) was quantified by spectrofluorimetry using horseradish peroxidase and homovanillic acid (excitation: 315 nm; emission: 425 nm) in 50 mM HEPES pH 7.5 (Romero-Puertas *et al.*, 2004b). A standard curve with known concentrations of commercial H_2O_2 was used to quantify samples. H_2O_2 accumulation was also imaged by confocal laser scanning microscopy (CLSM) using 2',7'-dichlorodihydrofluorescein diacetate (DCF-DA) in 10 mM Tris-HCl (pH 7.4). Leaf sections (2 mm^2) were incubated for 30 min with DCF-DA at 485 nm excitation and 530 nm emission (Terrón-Camero *et al.*, 2019) and were then embedded in 30% (w/v) polyacrylamide blocks. Leaf sections were cut

using a vibratome (Rodríguez-Serrano *et al.*, 2009) and analysed with the aid of a confocal laser scanning microscope (Leica TCS SL; Leica Microsystems). Chlorophyll-induced autofluorescence was also detected (excitation at 633 nm and emission at 680 nm).

Hormonal Analysis

Hormone extraction and analysis were carried out mainly as described in Balfagón et al. (2019). Before hormonal extraction, a mixture containing 50 ng of [$^{2}H_{6}$]-ABA, [C13]-SA and dihydrojasmonic acid was added to 0.1 g of dry tissue as internal controls and hormones were quantified using a TQ-S Micro Triple Quadrupole Mass Spectrometer.

Microarray Data Bioinformatics and Statistical Analysis

2,4-D- and DMSO/EtOH (control)-sprayed leaves of similar sizes and developmental stages were sampled at 1 and 72 h. For microarray analysis, three independent biological replicates, each composed of leaves pooled from at least 5 different plants, were used per experimental condition. As described previously (Rodríguez-Serrano *et al.*, 2009), isolated total RNA was treated with deoxyribonuclease I (DNaseI; Turbo DNA free, Thermo Fisher Scientific) and cleaned on RNeasy Mini columns (Qiagen). These RNA samples were used to perform chip hybridization and analysis of transcriptional measures (Arabidopsis ATH1 chips; Affymetrix, Santa Clara, CA, US) at the *Centro Nacional de Biotecnología* (CSIC, Madrid). Expression data were normalized using the Robust Multi-array Average (RMA) algorithm implemented in the affyPLM package. Differential gene expression was based on linear models for analysing microarray data (LIMMA) (Smyth and Speed, 2003). Both affyPLM and LIMMA are part of the Bioconductor project (Ihaka and Gentleman, 1996). Differentially expressed (DE) genes were obtained by paired comparisons, with two independent comparisons carried out for each combination of treated samples vs. control for each genotype. Only genes with a fold-change (FC) over 1.5 ($|\log2(FC)| > 0.58496$) and an adjusted $P < 0.05$ (adjusted using the false discovery rate (FDR) method developed by Benjamini-Hochberg) were considered for further investigation. The non-overlapping genes between the data

Comentado [MGCD1]: ¿NO será [^{13}C]-SA?

Comentado [MGCD2]: La cita de bioconductor es más reciente, de 2004 en Genome Biology: doi: 10.1186/gb-2004-5-10-r80 https://pubmed.ncbi.nlm.nih.gov/15461798/

Comentado [MGCD3]: Si queréis poner la referencia, es esta: Y.Benjamini and Y.Hochberg (1995): Controlling the false discovery rate: a practical and powerful approach to multiple testing. *Journal of the Royal Statistical Society, Series B (Methodological)*, **57**, 289-300.

sets of interest were computed using the Venny algorithm (http://bioinfogp.cnb.csic.es/tools/venny/).

Array data were deposited in …

Gene expression of relevant genes was confirmed by quantitative real-time polymerase chain reaction (qRT-PCR) as described elsewhere (Terrón-Camero *et al.*, 2020), where the relative expression of each gene was normalized to that of *TUB4*, and fold changes were calculated as $2^{-\Delta\Delta Ct}$ (Suppl. Fig. S2). Primers used in this study are described in Suppl. Table S1. RNA amplification, labelling and slide hybridization were essentially carried out as described in Adie et al. (2007).

ROSMETER and bioinformatic analyses

The ROSMETER platform was used to identify transcriptomic imprints in plant responses to 2,4-D on the basis of ROS type and origin (Rosenwasser *et al.*, 2013). ROS-producing treatments compiled in the ROSMETER platform are detailed in Suppl. Table S1 produced by Rosenwasser et al. (2013). Significantly enriched GO terms from data sets of interest were analysed using Mapman software (https://mapman.gabipd.org/), which displays large datasets in diagrams of metabolic pathways, and the classification SuperViewer tool on the BAR website (http://bar.utoronto.ca/ntools/cgi-bin/ntools_classification_superviewer.cgi), with automatically derived functional GO classifications, as of March 31, 2019, downloaded from the TAIR website (ATH_GO_GOSLIM.txt.gz, file ATH_GO_GOSLIM.txt). For functional protein association networks, the String database (https://string-db.org/) was used.

Statistical analysis

Mean values for the quantitative experiments described above were obtained from at least three independent experiments, with no less than three independent samples per experiment. Statistical analyses were performed using a two-way ANOVA test followed by a Tukey multiple comparison test ($P < 0.05$). The analyses were carried out with the aid of IBM SPPS Statistics 24 and GraphPad Prism 6. Error bars representing standard error (SEM) are shown in the figures.

Comentado [MGCD4]: Yo creo que no depositamos estos datos en ningún sitio... En cualquier caso, hay que depositar los CEL originales, no los análisis. Otra opción es compartirlo desde Zenodo, FigShare o cualquier otro servidor público. Lo que sí habría que incluir en el material complementario es la lista de genes que han pasado estos filtros en cada comparación.

Comentado [MGCD5]: La dirección http://app.agri.gov.il/noa/ROSMETER.php no funciona... Espero que no pidan un recálculo :-D

Comentado [MGCD6]: Esta tabla son cebadores, nada que ver con lo que entiendo que debería contener.

Comentado [MGCD7]: Hay que decir qué se considera estadísticamente signficativo. O sea, qué filtro de P o F se ha usado, y con qué programa.

Comentado [MGCD8]: Deberíais también especificar si la red se basa en todas las interacciones o habéis usado solo algunas, y qué valor de corte habéis considerado significativo (para descartar las interacciones poco contrastadas).

RESULTS

ACX1: a principal source of ROS following 2,4-D treatment in Arabidopsis

In a previous study carried out in our laboratory, concentrations of herbicide 2,4-D were optimized (Romero-Puertas *et al.*, 2004a; Rodríguez-Serrano *et al.*, 2014), with 23 mM 2,4-D being selected. ROS production has previously been found to increase 2,4-D treatment after 72 h, with some evidence suggesting that ACX, the enzyme catalysing the first step of β-oxidation, is an important source of 2,4-D-induced ROS (Pazmiño *et al.*, 2011). We firstly determined, in control and 2,4-D-treated WT plants, the expression levels of *ACX1*, which is induced under different abiotic stress and hormone supply conditions (Castillo *et al.*, 2004). The induction of *ACX1* in WT indicates that this enzyme may play a role in ROS production after herbicide treatment (Suppl. Fig. S2). To further study the role of ROS in plant responses to 2,4-D, we focused on the *acx1-2* mutant which is impaired in *ACX1* (Adham *et al.*, 2005). Phenotype and H_2O_2 production after 2,4-D treatment were characterized in WT and *acx1-2* plants (Fig. 1). The spraying of Arabidopsis WT plants with 23 mM 2,4-D produced pronounced epinasty in rosette leaves and leaf turgidity loss, reaching maximum levels after 72 h of treatment, as described elsewhere (Rodríguez-Serrano *et al.*, 2014; Fig. 1 A), while epinasty was less severe in the *acx1-2* mutant than in WT (Fig. 1 A). Homozygous *acx1-4* mutant, with a T-DNA insertion also in *ACX1*, showed similar responses to *acx1-2,* indicating that part of the phenotype observed in WT plants treated with 2,4-D may be due to *ACX1* (Suppl. Fig. S1 A-C). An increase in H_2O_2 in 2,4-D-treated WT plants as compared to untreated plants was fluorimetrically observed, which reached a peak after 1 h of treatment; however, the highest accumulation took place after 72 h of treatment (Fig. 1 B), while *acx1-2* mutant failed to accumulate H_2O_2 in response to 2,4-D, with a similar pattern being observed in control plants. Confocal microscopic detection of H_2O_2 corroborated these findings (Fig. 1 C), with a considerable reduction in H_2O_2-dependent fluorescence being observed after 72 h of 2,4-D treatment in *acx1-2* mutant as compared to WT plants (Fig. 1 C).

The herbicide 2,4-D generates an early transcriptome footprint related to peroxisomal stress.

Although part of the 2,4-D effect appears to be ROS-dependent (Grossmann *et al.*, 2001; Rodríguez-Serrano *et al.*, 2014; De *et al.*, 2016; Sandalio *et al.*, 2016), not much is known about the molecular mechanism underlying ROS-dependent regulation. Taking into account the clear relationship between H_2O_2 accumulation and the *acx1-2* phenotype in response to 2,4-D, we performed a time-course microarray analysis of WT and *acx1-2* Arabidopsis plants treated with 2,4-D to identify genes differentially regulated in both lines in response to the herbicide. We used two time points to detect early signalling plant responses: at 1h post treatment, which corresponds to a peak level of H_2O_2 in WT plants, and at 72 h post treatment, when 2,4-D effects on plants can be observed and repair mechanisms activated (Rodríguez-Serrano *et al.*, 2014). We then investigated the occurrence of ROS-related transcriptomic signatures in our transcriptome using the ROSMETER bioinformatics platform related to ROS type and origin (Rosenwasser *et al.*, 2013). Significantly, the highest transcriptome correlation values after 1 h of 2,4-D treatment were found in relation to the transcriptomes of catalase mutants (*cat2*) exposed to 3 and 8 h high light, in which peroxisomal H_2O_2 is accumulated (Vanderauwera *et al.*, 2005; Fig. 2 A), and in relation to the transcriptome obtained after treatment of WT with the catalase inhibitor 3-aminotriazole (AT), which also led to an increase in peroxisomal H_2O_2 (Gechev *et al.*, 2005; Fig. 2 A). The transcriptome also showed a significant correlation, although less than that observed with peroxisome-related transcriptomes obtained following direct applications of H_2O_2 in Arabidopsis seedlings (Davletova *et al.*, 2005), with the formation of superoxide being observed in the chloroplast and mitochondria after methyl viologen treatment (MV; Kilian *et al.*, 2007), and to a lesser extent with oxidative stress occurring after treatment with rotenone, a mitochondrial complex I inhibitor (Garmier *et al.*, 2008; Fig. 2 A). The correlation values for the *cat2* signature declined over time (72 h), while those related with other ROS origin increased (Fig. 2 B), suggesting that the contribution of other organelles such as mitochondria and chloroplasts in 2,4-D-induced ROS production occurs at a later stage (Fig. 2 B).

Comentado [MGCD9]: Yo no acabo de entender muy bien qué se representa en esta figura y entre qué cosas se hace la correlación.

Hormone levels in plant responses to 2,4-D

Epinasty is regulated by hormonal cross-talk (Sandalio *et al.*, 2016) and peroxisomal β-oxidation is required for the biosynthesis of certain hormones such as IAA and jasmonic acid (JA) (reviewed in Raghavan *et al.*, 2006; Sandalio and Romero-Puertas, 2015). We therefore further analysed different hormones in leaves from WT and *acx1-2* Arabidopsis plants treated or not with 2,4-D. Abscisic acid (ABA), which has been reported to be involved in 2,4-D toxicity (Raghavan *et al.*, 2006) and to regulate epinasty and hyponasty (Cox *et al.*, 2004), increased in plant responses to 2,4-D with the period of treatment, although no significant differences were observed in relation to *acx1-2* as compared to WT plants (Fig. 3 A). A significant increase in salicylic acid (SA) content was observed after 72 h of 2,4-D treatment, with slightly higher levels observed in *acx1-2* mutant than in WT (Fig. 3 B). On the other hand, we observed a significant decrease in JA concentrations in WT plants in response to 2,4-D treatment after 72 h, suggesting that JA may not be a key molecule for triggering epinasty following herbicide treatment. No changes in JA content were observed in *acx1-2* mutant after treatment, although this mutant showed predictably lower levels of JA with respect to WT in all cases (Fig. 3 C), as β-oxidation is required for JA synthesis to occur (Castillo *et al.*, 2004).

ACX1-dependent genes in early plant responses to 2,4-D

Peroxisomes appear to be one of the main targets for H_2O_2 accumulation in early plant responses to 2,4-D, with ACX1 appearing to be one of the principal sources of this accumulation. Transcriptome analysis thus provides a deeper insight into both WT and *acx1-2* mutant by identifying peroxisomal-dependent genes that regulate plant responses to the herbicide. Large sets of transcripts responded to 2,4-D treatment in the leaves of WT and *acx1-2* mutant at both time points analysed (Fig. 4 and Fig. 5). A comparison of these sets of transcripts between WT and *acx1-2* mutant revealed that, in the early response (1 h) of WT to 2,4-D stress, the number of gene transcripts regulated in the leaves of both WT and the mutant was around 3,600 (Fig. 4 A). However, 7,442, or double the number of genes as compared to that at the early response stage, were regulated at 72 hpt in WT, while in the *acx1-2* mutant, the number reached 8,309, almost 1,000 genes more than in WT (Fig. 5 A). To further study the role of ACX1-dependent H_2O_2 in the response of leaves to 2,4-D stress, we focused on changes

in the abundance of transcripts in the leaves of WT plants, but not in *acx1-2* mutant. These ACX1-dependent transcripts included 698 up-regulated and 644 down-regulated transcripts at 1 hpt (Fig. 4 B; Suppl. Table S2); and 841 up-regulated and 857 down-regulated transcripts at 72 hpt (Fig. 5 B; Suppl. Table S2). Early ACX1-dependent up-regulated transcripts showed significant values for signal transduction, transport, stress-response pathways, cell organization and biogenesis, mainly related to the endoplasmic reticulum (ER) and Golgi apparatus (Fig. 4 C). ACX1-dependent down-regulated transcripts include transcription, developmental processes, in addition to up-regulated pathways, signal transduction, as well as cell organization and biogenesis, mainly related to the chloroplast and plastid (Fig. 4 C). At a later stage, ACX1-dependent up-regulated transcripts included a significant representation of stress-response pathways, transcription, and other biological and developmental processes, which are mainly associated with the cell wall and plasma membrane (Fig. 5 C). Down-regulated transcripts at 72 hpt included DNA and RNA metabolism, cell organization and biogenesis, as well as electron transport and energy pathways and other cellular processes, in addition to responses to abiotic and biotic stimulus, which were also up-regulated and are mainly associated with ribosomes and cytosol (Fig. 5 C). Quantitative real-time polymerase chain reaction (qRT-PCR) was used to verify the expression pattern of selected genes of interest belonging to different categories: *ATP24a*, *HSP, PR-1* and the peroxisomal Ca-dependent solute carrier; similar results were obtained through microarray and qRT-PCR analyses, thus demonstrating the reliability of microarray analysis (Suppl. Fig. S2). *ATP24a* encoding a peroxidase was upregulated in WT plants by 2,4-D, while an opposite pattern was observed in *acx1-2* mutants; *HSP* encoding a heat shock protein was upregulated in WT, but down-regulated in *acx1-2* mutant. At 72 hpt, similar results described at 1hpt were observed for *ATP24a* and *HSP,* while *PR-1* was upregulated in WT and to a lesser extent in *acx1-2*. The peroxisomal Ca-dependent solute carrier was down-regulated in WT and slightly up-regulated in *acx1-2* mutant.

Auxin signalling in plant responses to 2,4-D is ACX1-dependent

In the principal categories significantly represented in ACX1-dependent genes regulated by 2,4-D stress, we found genes associated with auxin

biosynthesis, metabolism and signalling (Table 1). We obtained a deeper insight into these genes given that epinasty and auxins are closely related (Qin *et al.*, 2005; Sandalio *et al.*, 2016; Ueda *et al.*, 2018). We then looked for available mutants affected in genes potentially regulated by peroxisomal ACX1-dependent H_2O_2 in response to 2,4-D associated with auxins (Table 1) in the 6,760 T-DNA mutant collection from the SALK Institute (NASC, ID: N27941). We found 21 mutants available (Table 1) and after 2,4-D treatment, the SALK_068787C mutant showed a similar epinasty phenotype to that of *acx1-2* mutant (Fig. 6). SALK_068787C mutant has a T-DNA insertion in the At1g12820 gene coding for protein AUXIN SIGNALING F-BOX 3 (AFB3; Fig. 6 A), so we named *afb3-1*. *AFB3* expression in WT and *acx1-2* mutants after 2,4-D treatment was validated by qRT-PCR, which showed a significant inhibition in WT, with no significant changes observed in *acx1-2* mutant (Fig. 6 C, Suppl. Fig. S2). We then determined the homozygosity of *afb3-1* (Fig. 6 B) and analysed *AFB3* expression under 2,4-D treatment conditions in this mutant (Fig. 6 B-C). We performed semiquantitative RT-PCR, which found no *AFB3* expression in *afb3-1* seedlings under our experimental conditions (Fig. 6 C). The AFB3 component of SCF (ASK-cullin-F-box) E3 ubiquitin ligase complexes acts as an auxin receptor which mediates Aux/IAA protein proteasomal degradation. Following String database enrichment analysis, setting no more than 10 interactors in the first shell, AFB3 was linked to auxin-regulated gene transcription and directly linked to the S-phase kinase-associated protein (Skp) (Fig. 7 A, Table 2), which acts as an adapter that connects the F-box protein to CUL1. A similar result was obtained setting five interactors in a second shell (Fig. 7 B). In fact, ubiquitin-dependent degradation was induced after 2,4-D treatment of ACX1-dependent genes, mainly at 72 hpt, as imaged by Mapman software (Suppl. Fig. S3, Suppl. Table S3).

DISCUSSION

The action mode of auxinic herbicides such as 2,4-D is beginning to be understood more clearly. At high concentrations, 2,4-D has an inhibitory effect on growth and development, as well as growth abnormalities such as epinasty, leaf abscission and senescence (Grossmann, 2000; Pazmiño *et al.*, 2011; Sandalio *et al.*, 2016). Although most analysis of 2,4-D toxicity has focused on

the event cascade involving ethylene and ABA induction, ROS has been reported to play a central role in the development of the main effects of 2,4-D, including epinasty and senescence (Pasternak *et al.*, 2005; Pazmiño *et al.*, 2011; Sandalio *et al.*, 2016). In fact, the tolerance of *Salvinia natan* to 2,4-D is related to its capacity to cope with oxidative stress (Dolui *et al.*, 2021). Although the 2,4-D-dependent phenotype and certain biochemical issues have been characterized in different plant species, less information is available at the molecular level. Transcriptomic analyses of short-term treatment of Arabidopsis plants with 2,4-D (1 h) have revealed significant changes in the transcription levels of genes belonging to the functional categories of transcription, metabolism, cellular communication, signal transduction, subcellular localisation, transport facilitation, protein fate, proteins with binding functions or cofactor requirements, as well as cellular environmental regulation/interactions (Raghavan *et al.*, 2005). As described by Raghavan et al. (2005, 2006), 2,4-D not only modulates the expression of auxin, ethylene and abscisic acid (ABA) pathways but also regulates a wide variety of other cellular processes including rescue, defence and pathogen-related gene functions (Raghavan *et al.*, 2005). Comparative analyses of IAA- and 2,4-D-induced transcriptomes have shown similar differential gene expression patterns (Pufky *et al.*, 2003; Raghavan *et al.*, 2005, 2006; McCauley *et al.*, 2020). Most of these studies have focused on genes associated with the metabolism and signalling of other plant hormones including abscisic acid (ABA) and ethylene, which are assumed to play a fundamental role in triggering plant death following auxin herbicide treatment (Raghavan *et al.*, 2005, 2006; Gaines *et al.*, 2020; McCauley *et al.*, 2020). However, whether and how H_2O_2 modulates auxin and 2,4-D transcriptional responses, as well as the sources of ROS involved, have not been elucidated. Some evidence suggests that ACX is an important source of ROS induced by the herbicide 2,4-D (Pazmiño *et al.*, 2011). In Arabidopsis, ACX is a family of six enzymes with overlapping specificities for acyl-CoA substrates of various chain lengths (Schilmiller *et al.*, 2007; Khan *et al.*, 2012). ACX1 shows specificity for medium- to long-chain acyl-CoA (C12:0 to C16:0) substrates; ACX2 preferentially uses long-chain saturated and unsaturated acyl-CoAs (C14:0 to C20:0); while ACX3 shows medium-chain length substrate specificity (C8:0 to C14:0). ACX4 displays specificity for short-chain acyl-CoAs substrates (C4:0 to C8:0), while the fatty acyl-CoA substrate

specificity and biological functions of ACX5 and ACX6 are currently unknown (Eastmond *et al.*, 2000). In this study, *acx1* mutants showed a noteworthy reduction in epinasty in response to 2,4-D. In addition, analysis and imaging of H_2O_2 accumulation clearly show that ACX1 is the main source of ROS under 2,4-D treatment conditions (Fig. 1). It is therefore possible to conclude that the epinastic phenotype is mainly associated with ACX1-dependent H_2O_2 in accordance with the 2,4-D-dependent induction of ACX activity previously observed in pea leaves (Pazmiño *et al.*, 2011) and *ACX1* induction observed in this study (Suppl. Fig. S2). Evidence at the biochemical and molecular levels has demonstrated that high exogenous concentrations of 2,4-D alter plant hormone levels, contributing to the epinasty phenotype and senescence (Raghavan *et al.*, 2005, 2006; Sandalio *et al.*, 2016). However, analyses of ABA, JA and SA in both WT and *acx1-2* mutant suggest that these molecules do not play a key role in the regulation of epinasty under our experimental conditions.

In a previous study, epinasty was shown to be the result of differential ROS accumulation in leaves and of changes in the actin cytoskeleton caused by ROS- and NO-dependent posttranslational modifications of actin (Rodríguez-Serrano *et al.*, 2014); the reduction of H_2O_2 in *acx1-2* mutant could therefore explain the considerable reduction in epinasty observed in this Arabidopsis line. However, H_2O_2 is a signalling molecule involved in the regulation of cell responses to biotic and abiotic stress conditions (Fichman and Mittler, 2020). Interestingly, time course analysis of H_2O_2 in WT leaf extracts showed a clear peak at 1 hpt and further increases during the period of 2,4-D exposure. We therefore analysed gene expression after 1 hpt and 72 hpt in both WT and *acx1-2* mutant to identify genes differentially regulated in early and long-term responses to 2,4-D. The specific induction of genes at the early stage of 2,4-D exposure constitutes the primary response which can even regulate cellular events induced at a later stage. A similar number of early genes regulated by 2,4-D was observed in WT and *acx1-2* mutant, and the *ACX1*-dependent transcripts identified were related to signal transduction, transport, stress-response pathway, cell organization and biogenesis categories. The results obtained by transcriptomic analyses were verified by qRT-PCR analysis of several genes belonging to different categories, with similar results obtained by both approaches. Among the early-response genes analysed, peroxidase-encoding *ATP24a* was down-

regulated by 2,4-D in *acx1-2* mutant. *ATP24a* is involved in removing H_2O_2, toxic reductant oxidation, lignin biosynthesis, degradation, suberization, auxin catabolism and responses to environmental stresses such as wounding, pathogen attack and oxidative stress, although these functions might be dependent on each isozyme/isoform in each plant tissue (https://www.genscript.com/protein-database/per62_arath). Changes in the peroxidase pattern induced by 2,4-D have been reported in the cotyledon cell suspension cultures of bush bean, while peroxidase activity, which has been suggested to correlate with cell wall expansion, may play a role in cell growth (Arnison and Boll, 1978). *HSP* and PR-1 were down-regulated in *acx1-2* mutant but upregulated in WT after treatment with 2,4-D. HSPs were differentially expressed at the transcriptional level, and protein content was up-regulated after 24 and 72 hpt in citrus fruits under 2,4-D treatment (Ma *et al.*, 2014). HSPs could prevent irreversible protein inactivation and aggregation and, acting as chaperonins, could favour protein transport (Pazmiño *et al.*, 2011). *HSP71.2* and *PRP4A* expression was up-regulated in pea plants in response to 2,4-D and both genes were regulated by ROS (Pazmiño *et al.*, 2011), thus supporting differential expression in *acx1-2*.

We then focused our attention on auxin-related genes (Table 1). Early-response genes up-regulated by 2,4-D specifically in WT and not in *acx1-2* mutant (*ACX1*-dependent genes) are involved in auxin stimulus (i.e.: *IAA10*, *IAA26* and *RCE1_RUB1 conjugating enzyme 1)*, and in the cellular response to auxin stimulus (i.e: *SGT1A* phosphatase-like proteins; Table 1). On the other hand, *ACX1*-dependent genes down-regulated by 2,4-D included genes related to polar and basipetal auxin transport (i.e.: *HSL1_HAESA-like 1; ABCB14 and D6PK*), regulation of auxin mediated signalling pathways (i.e.: *PIF5_PIL6_phytochrome interacting factor 3-like 6, TIR1_F-box/RNI-like superfamily protein, AFB5_auxin F-box protein 5, AFB3_auxin signaling F-box 3, SAUR*; Table 1). Most of these genes have been identified as early auxin-response genes in different plant species (Abel and Theologis, 1996), such as Arabidopsis (Raghavan *et al.*, 2005, 2006) and citrus fruits (Ma *et al.*, 2014) exposed to 2,4-D. These results demonstrate that 2,4-D acts through auxin-signalling pathways and that peroxisomal ACX1 plays an important role in regulating early auxin-signalling responses to 2,4-D involved in the epinasty phenotype. Interestingly, longer exposure to 2,4-D (72h) affected twice the

number of genes as compared to early responses, with the highest numbers observed in *acx1-2. ACX1*-dependent genes regulated after long periods of 2,4-D exposure are associated with stress-response pathways, transcription and developmental processes and are mainly related to the cell wall and plasma membrane; this suggests that longer periods of treatment preferentially activate repair and defence mechanisms to cope with damage induced by the herbicide. However, long term 2,4-D exposure also up-regulates auxin-related genes, most of which correlate with the response to auxin stimulus (i.e.: MYB domain proteins, *MYB6 and MYB109*, *arginine decarboxylase 2 ADC2 and SGT1 phosphatase-related protein*), and down-regulated auxin-related genes including the SAUR-like auxin-responsive protein family and *IAA8*. Analysis of the transcriptome in WT and *acx1-2* using the bioinformatic tool ROSMETER shows a high correlation with peroxisomal H_2O_2 production during the first hour of treatment, thus suggesting that peroxisomal ACX1-dependent H_2O_2 plays an important role as a signalling molecule in the regulation of rapid responses to the herbicide. Meanwhile, longer periods of treatment reduce the correlation with peroxisomal ROS, while the correlation with other sources such as mitochondria and chloroplasts was found to increase; this suggests the generation of progressive waves of different types of ROS involving different organelles, which also stimulates multiple signal sources. Oxidative stress characterized by ROS overaccumulation and lipid peroxidation has been associated with 2,4-D-dependent leaf epinasty and senescence symptoms in different plant species (Karuppanapandian *et al.*, 2011; Pazmiño *et al.*, 2011), although the contribution of different sources of ROS and organelles have not been explored in great depth.

2,4-D has been reported to be a poor substrate for ABP1, a disputed potential auxin receptor (Gao *et al.*, 2015), whose action mode is thought to be through the nuclear-localized TIR1/AFB auxin receptors, which promote the degradation of Aux/IAA transcriptional repressors in an auxin-dependent manner via the ubiquitin-proteasome system (UPS) (Parry *et al.*, 2009; Eyer *et al.*, 2016). In fact, 2,4-D has been reported to have an inhibitory effect on plant growth via the TIR1/AFB auxin-mediated signalling pathway (Eyer *et al.*, 2016). Screening of available mutants related to *ACX1*-dependent genes in plant responses to 2,4-D (Table 1) showed that *afb3-1,* with a T-DNA insertion in *AFB3,* which has a similar phenotype to that of *acx1-2* and *acx1-4* in response to 2,4-D, appears to

play a key role in developing epinasty and could be regulated by ROS. In addition, analysis of AFB3 using the String database shows a close relationship with genes directly connected with auxins and ubiquitin-dependent degradation, which, in turn, is induced by 2,4-D, mainly after longer exposure to the herbicide, as we found after Mapman analysis. At this time point, protein degradation related to the E3-RING ubiquitin ligase and S-phase kinase associated with the protein 1 (SKP1) Cullin F-box E3-ligase (SCF)$^{TIR1/AFB}$ complex is significantly regulated (Suppl. Fig. S3 and Suppl. Table S3).

SCF $^{TIR1/AFB}$ contains interchangeable F-box proteins (FBPs) which determine the specificity to the E3 protein through direct physical interactions with the targets to be degraded (Hua and Vierstra, 2011). At high IAA levels, TIR1/AFB 1–5 increase the affinity for the AUX/IAA degron through direct IAA binding, resulting in AUX/IAA ubiquitylation and further degradation, thus ensuring ARF derepression and auxin-induced transcriptional changes (Calderon Villalobos et al, 2012; Fig. 8). Several studies have highlighted the distinct biochemical properties and biological functions of AFBs, with TIR1/AFB2 showing stronger interactions with Aux/IAA than AFB1 and AFB3; AFB3 has been shown to play a role in responses to nitrate and salinity (Calderón Villalobos et al, 2012; Garrido Vargas et al, 2020). Our results show that AFB3 expression is regulated by H_2O_2 produced by ACX1 whose silencing could interfere with AUX/IAA ubiquitinilation and degradation and reduce the epinasty phenotype as observed in *acx1* mutants. This finding is corroborated by the similar phenotype observed in af*b3-1* mutants. However, the silencing of AFB3 does not completely prevent leaf epinasty, suggesting that other complex factors, such as the reported necessity of TIR1 for 2,4-D perception (Calderon-Villalobos et al. 2010) and the resistance of *tir1* mutants to 2,4-D (Parry et al. 2009), are involved.

Comentado [MGCD10]: En esta figura es muy difícil apreciar las diferencias antre la parte A y la B, que solo parece estar en el rectángulo de expresiones. Yo creo que es muy útil para entender la discusión y habría que pasarla a una figura del artículo, siempre que se resalte un poco más el efecto, o que se elija solo uno de los tiempos.

CONCLUSIONS

Reactive oxygen species (ROS) are involved in the toxicity of auxinic 2,4-D and most of the characteristic phenotypes associated with this herbicide. However, peroxisomal ROS derived from ACX1 also play an important role in signalling in response to 2,4-D and regulate a large number of genes, such as peroxidases, HSP and PRPs, involved in primary responses to 2,4-D.

Additionally, ACX1-dependent H_2O_2, which regulates *AFB3* expression, can modulate AUX/IAA ubiquitination and degradation and thereby the expression of auxin-responsive genes (Fig. 8). However, longer periods of 2,4-D treatment produce different waves of ROS production associated with chloroplasts and mitochondria which regulate stress-response pathways, transcription and developmental processes, suggesting that repair and defence mechanisms are activated to cope with damage induced by the herbicide. Further analysis is necessary to determine the additional roles played by ACX1-dependent H_2O_2 in the regulation of cell responses to IAA and the 2,4-D herbicide.

ACKNOWLEDGEMENTS

This study was funded by the Spanish Ministry of Science, Innovation and Universities (MCIU), the State Research Agency (AEI) and FEDER grant PGC2018-098372-B-I00. MAP-V was supported by MCIU Research Personnel Training (FPI) grant BES-2016-076518. The authors also wish to thank Michael O'Shea for proofreading the manuscript.

Conflict of interest: The authors declare no conflict of interest.

Figure legends

Figure 1. Effect of 2,4-D on plant phenotype and ROS production. A) WT and *acx1-2* plants were foliarly treated with 23 mM 2,4-D, whose phenotypic impact is shown (72 h). B) H_2O_2 content fluorimetrically assayed in acid extracts from WT and *acx1-2* leaves after plant spraying with 2,4-D (1h-72h). Values are means ± SE of at least three experiments with three independent extracts each. C) Confocal laser scanning microscopy (CLSM) imaging of H_2O_2 accumulation in cross-sections of Arabidopsis leaves using DCF-DA (Ex/Em: 485/530 nm). Images are maximal projections from several optical sections and are representative of at least 15 leaf sections from four different experiments. Different letters denote significant differences between 2,4-D treatment time points within the same genotype, obtained using Tukey multiple comparison tests (p-value < 0.05). The absence of letters indicates no significant differences. Asterisks denote significant differences between treated *acx1-2* and WT plants at each time point according to the Student´s t-test (p-value < 0.05). The absence of

an asterisk denotes no significant differences between *acx1-2* and WT plants under control conditions. e, epidermis; mc, mesophyll cells; st, stomata; x, xylem.

Figure 2. Analysis of 2,4-D transcriptome using the ROSMETER platform. Correlation values of changes in the transcriptome in WT Arabidopsis plants treated with 2,4-D for 1h (A) and 72h (B) generated by the ROSMETER platform. Correlation values (*y* axis ordinate) were obtained as described by Rosenwasser et al. (2011, 2013) from the 2,4-D transcriptome and transcriptomes of the individual ROS-producing treatments compiled in the ROSMETER platform (*x* axis abscissa) detailed in Suppl. Table S1 produced by Rosenwasser et al (2013). 1 indicates complete correlation. Positive and negative data correspond to positive and negative correlation, respectively, between the transcriptomes. 0 indicates no correlation. Correlation values above 0.4 (discontinuous line) can be considered significant correlation values that provide biological insights (Rosenwasser et al., 2013). Higher correlation values (arrows) at 1 h relate to peroxisomal stress (AT, aminotriazol treatment) cat_3h and cat_8h, *cat2-2* mutants under 3 and 8 h high light stress, respectively. Higher correlation values (arrows) at 72 h relate to peroxisomal stress (AT, aminotriazol treatment), general stress (methyl viologen, MV 6h treatment), chloroplast stress (*fnr*1 mutants) and mitochondrial stress (*aox* mutants).

Figure 3. Effect of 2,4-D on plant hormone production. A) ABA, B) SA and C) JA production in WT and *acx1-2* plants after 2,4-D spraying at 1h and 72 h. Amplification of the graph at 0 and 1 h treatment in A). Bars represent the mean ± SE of at least 4 replicates. Different letters denote significant differences between the different values obtained using Tukey multiple comparison tests (p-value < 0.05).

Figure 4. Changes in global transcript expression in the *acx1-2* mutant compared to wild type (WT) in response to short-term 2,4-D treatment. A) Number of up- and down-regulated genes in WT and *acx1-2* mutants after 1 h of 2,4-D spraying, and Venn diagrams B) showing the overlap between gene expression changes in WT and *acx1-2* mutants after 1 h of 2,4-D spraying; upregulated transcripts at the top and downregulated transcripts at the bottom. Transcript expression altered in the leaves of WT plants, but not of *acx1-2* mutants (ACX1-dependent) is marked by blue (up-regulated) and orange (down-regulated) coloured stripes. Five main categories after gene ontology (GO)

enrichment of ACX1-dependent up- (C) and down- (D) regulated transcripts after 1h of 2,4-D spraying. Normed to frequency of class over all ID numbers on *x* axes.

Figure 5. Changes in global transcript expression in the *acx1-2* mutant as compared to wild type (WT) in response to long-term 2,4-D treatment. A) Number of up- and down-regulated genes in WT and *acx1-2* mutants after 72 h of 2,4-D spraying, and Venn diagrams B) showing the overlap between gene expression changes in WT and *acx1-2* mutants after 72 h of 2,4-D spraying; up-regulated transcripts on top and down-regulated transcripts on bottom. Transcript expression altered in leaves of WT plants, but not in *acx1-2* mutants (ACX1-dependent), is marked by blue (up-regulated) and orange (down-regulated) coloured stripes. Five main categories after gene ontology (GO) enrichment of ACX1-dependent up- (C) and down- (D) regulated transcripts after 72h of 2,4-D spraying. Normed to frequency of class over all ID numbers on *x* axes.

Figure 6: *afb3-1* genotyping and *AFB3* expression in plants treated with 2,4-D. A) Diagram showing the position of the T-DNA insertion and primers used (LP, RP and LBb1.3) for genotyping *afb3-1* mutant; B) PCR-based genotyping of WT and mutant plants. Ethidium bromide stained amplicons obtained when using LP, RP and LBb1.3 primers; C) Semi-quantitative RT-PCR analysis of *AFB3* transcript in WT and *afb3-1* leaves after 1 and 7 h of spraying with 2,4-D. No amplification of the transcript was observed following quantitative analysis of *afb3-1* mutants. D) WT, *afb3-1* and *acx1-2* plants were foliarly treated with 23 mM 2,4-D, whose effect on leaves phenotype is shown. Leaves were sliced after 72 h of 2,4-D spraying to better view epinasty.

Figure 7: Predicted functional partners of AFB3. SKP1-like proteins involved in ubiquitination and subsequent proteasomal degradation of target proteins obtained using the stringDB tool (https://string-db.org/) following the selection of no more than 10 interactors (A) are the main partners of AFB3. Together with CUL1, RBX1 and AFB3, SKPs forms a SCF E3 ubiquitin ligase complex in which SKPs act as adapters linking AFB3 to CUL1. Similar results including five interactors in a second shell were obtained (B).

Figure 8: Scheme showing the possible mechanistic toxicity of 2,4-D in Arabidopsis plants. At high IAA levels, TIR1/AFB 1–3 increase the affinity for the AUX/IAA degron through direct IAA binding, resulting in AUX/IAA

ubiquitination and further degradation, thus ensuring ARF de-repression and auxin-induced transcriptional changes. ACX1-dependent H_2O_2 is involved in the toxicity of the auxinic herbicide 2,4-D, regulating *AFB3* expression, thus enabling ubiquitination and degradation of AUX/IAA, leading to the modulation of auxin-responsive gene expression.

Supplementary Material

Suppl. Fig. S1: ***acx1-4* genotype and phenotype in plants treated with 2,4-D.** A) Diagram showing the position of the T-DNA insertion and primers used (LP, RP and LBb1.3) for genotyping *acx1-4* mutants. B) PCR-based genotyping of WT and mutant plants. Ethidium bromide-stained amplicons obtained when using LP, RP and LBb1.3 primers. C) WT and *acx1-4* plants were foliarly treated with 23 mM 2,4-D whose effect on the leaf phenotype is shown.

Suppl. Fig. S2: **Validation of microarray results.** Quantitative real-time PCR compared with fold change (FC) data obtained by microarray analyses of genes related to different categories. FCs using qRT-PCR were calculated as $2^{-\Delta\Delta Ct}$ (n= 3). Primers used are described in Supplemental Table S1. Each gene was normalized against *TUB4* expression.

Suppl. Fig. S3: **Diagram of ACX1-dependent genes regulated by 2,4-D relating to ubiquitin-dependent degradation using MapMan.** A) After 1h of 2,4-D treatment; B) after 72h of 2,4-D treatment. At 72 hpt, protein degradation related to E3-RING and E3-SCF-FBOX ubiquitin categories (Suppl. Table S3), was significantly regulated.

Suppl. Table S1: Reverse transcription quantitative PCR and genotyping primers.

Suppl. Table S2: ACX1-dependent genes regulated after 2,4-D treatment at 1 and 72hpt.

Suppl. Table S3: ACX1-dependent categories and genes regulated after 2,4-D treatment at 72hpt related to ubiquitin-dependent degradation (Suppl. Fig. S3 B).

Reference List

Abel S, Theologis A. 1996. Early genes and auxin action. Plant Physiology **111**, 9–17.

Adham AR, Zolman BK, Millius A, Bartel B. 2005. Mutations in Arabidopsis acyl-CoA oxidase genes reveal distinct and overlapping roles in β-oxidation. Plant Journal **41**, 859–874.

Adie BAT, Pérez-Pérez J, Pérez-Pérez MM, Godoy M, Sánchez-Serrano JJ, Schmelz EA, Solano R. 2007. ABA is an essential signal for plant resistance to pathogens affecting JA biosynthesis and the activation of defenses in Arabidopsis. Plant Cell **19**, 1665–1681.

Arnison PG, Boll WG. 1978. The effect of 2,4-D and kinetin on the activity and isoenzyme pattern of various enzymes in cotyledon cell suspension cultures of bush bean (*Phaseolus vulgaris* cv. Contender). Canadian Journal of Botany **56**, 2185–2195.

Balfagón D, Sengupta S, Gómez-Cadenas A, Fritschi FB, Azad RK, Mittler R, Zandalinasc SI. 2019. Jasmonic acid is required for plant acclimation to a combination of high light and heat stress. Plant Physiology **181**, 1668–1682.

Burns CJ, Swaen GMH. 2012. Review of 2,4-dichlorophenoxyacetic acid (2,4-D) biomonitoring and epidemiology. Critical Reviews in Toxicology **42**, 768–786.

Calderón Villalobos, L. I. et al. A combinatorial TIR1/AFB-Aux/IAA co-receptor system for differential sensing of auxin. Nat. Chem. Biol. 8, 477–485 (2012)

Castillo MC, Martínez C, Buchala A, Métraux JP, Léon J. 2004. Gene-specific involvement of β-oxidation in wound-activated responses in Arabidopsis. Plant Physiology **135**, 85–94.

Cox MCH, Benschop JJ, Vreeburg RAM, Wagemaker CAM, Moritz T, Peeters AJM, Voesenek LACJ. 2004. The roles of ethylene, auxin, abscisic acid, and gibberellin in the hyponastic growth of submerged *Rumex palustris* petioles. Plant Physiology **136**, 2948–2960.

Davletova S, Rizhsky L, Liang H, Shengqiang Z, Oliver DJ, Coutu J, Shulaev V, Schlauch K, Mittler R. 2005. Cytosolic ascorbate peroxidase 1 is a central component of the reactive oxygen gene network of Arabidopsis. Plant Cell **17**, 268–281.

De AK, Dey N, Adak MK. 2016. Some physiological Insights of 2,4-D sensitivity in an aquatic fern: *Azolla pinnata* R.Br. Journal of Biotechnology and Biomaterials **6**, 235.

Dolui D, Saha I, Adak MK. 2021. 2, 4-D removal efficiency of *Salvinia natans* L. and its tolerance to oxidative stresses through glutathione metabolism under induction of light and darkness. Ecotoxicology and Environmental Safety **208**, 111708.

Eastmond PJ, Hooks M, Graham A. 2000. The Arabidopsis acyl-CoA oxidase gene family Identification of Arabidopsis ACX isogenes Biochemical properties Gene expression and enzyme activity **28**, 755–757.

Egan JF, Maxwell BD, Mortensen DA, Ryan MR, Smith RG. 2011. 2,4-dichlorophenoxyacetic acid (2,4-D)-resistant crops and the potential for evolution of 2,4-D-resistant weeds. Proceedings of the National Academy of Sciences of the United States of America **108,** E37.

Enders TA, Strader LC. 2015. Auxin activity: past, present, and future. American Journal of Botany **102**, 180–196.

Eyer L, Vain T, Pařízková B, *et al.* 2016. 2,4-D and IAA amino acid conjugates show distinct metabolism in Arabidopsis. PLoS ONE **11**, 1–18.

Fichman Y, Mittler R. 2020. Rapid systemic signaling during abiotic and biotic stresses: is the ROS wave master of all trades? Plant Journal **102**, 887–896.

Gaines TA, Duke SO, Morran S, Rigon CAG, Tranel PJ, Anita Küpper, Dayan FE. 2020. Mechanisms of evolved herbicide resistance. Journal of Biological Chemistry **295**, 10307–10330.

Gao Y, Zhang Y, Zhang D, Dai X, Estelle M, Zhao Y. 2015. Auxin binding protein 1 (ABP1) is not required for either auxin signaling or Arabidopsis development. Proceedings of the National Academy of Sciences of the United States of America **112**, 2275–2280.

Garmier M, Carroll AJ, Delannoy E, Vallet C, Day DA, Small ID, Millar AH. 2008. Complex I dysfunction redirects cellular and mitochondrial metabolism in Arabidopsis. Plant Physiology **148**, 1324–1341.

Overexpression of the Auxin Receptor AFB3 in

Arabidopsis Results in Salt Stress Resistance and

the Modulation of NAC4 and SZF1

Fernanda Garrido-Vargas 1, Tamara Godoy 2, Ricardo Tejos 2 and José Antonio O'Brien Int. J. Mol. Sci. 2020, 21, 9528; doi:10.3390/ijms21249528

Gechev TS, Minkov IN, Hille J. 2005. Hydrogen peroxide-induced cell death in Arabidopsis: transcriptional and mutant analysis reveals a role of an oxoglutarate-dependent dioxygenase gene in the cell death process. IUBMB Life **57**, 181–188.

Grossmann K. 2000. Mode of action of auxin herbicides: a new ending to a long, drawn out story. Trends in Plant Science **5**, 506–508.

Grossmann K, Kwiatkowski J, Tresch S. 2001. Auxin herbicides induce H_2O_2 overproduction and tissue damage in cleavers (*Galium aparine* L.). Journal of Experimental Botany **52**, 1811–1816.

Hua, Z. & Vierstra, R. D. The cullin-RING ubiquitin-protein ligases. Annu.

Rev. Plant Biol. 62, 299–334 (2011).

Ihaka R, Gentleman R. 1996. R: a language for data analysis and graphics. Journal of Computational and Graphical Statistics **5**, 299–314.

Kao YT, Gonzalez KL, Bartel B. 2018. Peroxisome function, biogenesis, and dynamics in plants. Plant Physiology **176**, 162–177.

Karuppanapandian T, Wang HW, Prabakaran N, Jeyalakshmi K, Kwon M, Manoharan K, Kim W. 2011. 2,4-dichlorophenoxyacetic acid-induced leaf senescence in mung bean (*Vigna radiata* L. Wilczek) and senescence inhibition by co-treatment with silver nanoparticles. Plant Physiology and Biochemistry **49**, 168–177.

Khan BR, Adham AR, Zolman BK. 2012. Peroxisomal Acyl-CoA oxidase 4 activity differs between Arabidopsis accessions. Plant Molecular Biology **78**, 45–58.

Kilian J, Whitehead D, Horak J, Wanke D, Weinl S, Batistic O, D'Angelo C, Bornberg-Bauer E, Kudla J, Harter K. 2007. The AtGenExpress global stress expression data set: protocols, evaluation and model data analysis of UV-B light, drought and cold stress responses. Plant Journal **50**, 347–363.

Li ZF, Dong JX, Vasylieva N, Cui YL, Wan DB, Hua XD, Huo JQ, Yang DC, Gee SJ, Hammock BD. 2021. Highly specific nanobody against herbicide 2,4-dichlorophenoxyacetic acid for monitoring of its contamination in environmental water. Science of the Total Environment **753**, 141950.

Liszkay A, van der Zalm E, Schopfer P. 2004. Production of reactive oxygen intermediates ($O_2^{\cdot-}$, H_2O_2, and $^{\cdot}OH$) by maize roots and their role in wall loosening and elongation growth. Plant Physiology **136**, 3114–3123.

Ma Q, Ding Y, Chang J, Sun X, Zhang L, Wei Q, Cheng Y, Chen L, Xu J, Deng X. 2014. Comprehensive insights on how 2,4-dichlorophenoxyacetic acid retards senescence in post-harvest citrus fruits using transcriptomic and proteomic approaches. Journal of Experimental Botany **65**, 61–74.

McCauley CL, McAdam SAM, Bhide K, Thimmapuram J, Banks JA, Young BG. 2020. Transcriptomics in *Erigeron canadensis* reveals rapid photosynthetic and hormonal responses to auxin herbicide application. Journal of Experimental Botany **71**, 3701–3709.

Olmedilla A, Sandalio LM. 2019. Selective autophagy of peroxisomes in plants: from housekeeping to development and stress responses. Frontiers in Plant Science **10**, 1–7.

Pan R, Liu J, Wang S, Hu J. 2020. Peroxisomes: versatile organelles with diverse roles in plants. New Phytologist **225**, 1410-1427.

Parry G, Calderon-Villalobos LI, Prigge M, Peret B, Dharmasiri S, Itoh H, Lechner E, Gray WM, Bennett M, Estelle M. 2009. Complex regulation of the TIR1/AFB family of auxin receptors. Proceedings of the National Academy of Sciences of the United States of America **106**, 22540–22545.

Pasternak T, Potters G, Caubergs R, Jansen MAK. 2005. Complementary interactions between oxidative stress and auxins control plant growth responses at plant, organ, and cellular level. Journal of Experimental Botany **56**, 1991–2001.

Pazmiño DM, Rodríguez-Serrano M, Romero-Puertas MC, Archilla-Ruiz A, del Río LA, Sandalio LM. 2011. Differential response of young and adult leaves to herbicide 2,4-dichlorophenoxyacetic acid in pea plants: role of reactive oxygen species. Plant, Cell and Environment **34**, 1874–1889.

Pazmiño DM, Rodríguez-Serrano M, Sanz M, Romero-Puertas MC, Sandalio LM. 2014. Regulation of epinasty induced by 2,4-dichlorophenoxyacetic acid in pea and Arabidopsis plants. Plant Biology **16**, 809–818.

Pazmiño DM, Romero-Puertas MC, Sandalio LM. 2012. Insights into the toxicity mechanism of and cell response to the herbicide 2,4-D in plants. Plant Signaling and Behavior **7**, 425-427.

Prigge MJ, Greenham K, Zhang Y, Santner A, Castillejo C, Mutka AM, O'Malley RC, Ecker JR, Kunkel BN, Estelle M. 2016. The Arabidopsis auxin receptor F-box proteins AFB4 and AFB5 are required for response to the synthetic auxin picloram. G3: Genes, Genomes, Genetics **6**, 1383–1390.

Pufky J, Qiu Y, Rao M V., Hurban P, Jones AM. 2003. The auxin-induced transcriptome for etiolated Arabidopsis seedlings using a structure/function approach. Functional and Integrative Genomics **3**, 135–143.

Qin G, Gu H, Zhao Y, *et al.* 2005. An indole-3-acetic acid carboxyl methyltransferase regulates Arabidopsis leaf development. Plant Cell **17**, 2693–2704.

Raghavan C, Ong EK, Dalling MJ, Stevenson TW. 2005. Effect of herbicidal application of 2,4-dichlorophenoxyacetic acid in Arabidopsis. Functional and Integrative Genomics **5**, 4–17.

Raghavan C, Ong EK, Dalling MJ, Stevenson TW. 2006. Regulation of genes associated with auxin, ethylene and ABA pathways by 2,4-dichlorophenoxyacetic acid in Arabidopsis. Functional and Integrative Genomics **6**, 60–70.

Rinaldi MA, Patel AB, Park J, Lee K, Strader LC, Bartel B. 2016. The roles of β-oxidation and cofactor homeostasis in peroxisome distribution and function in *Arabidopsis thaliana*. Genetics **204**, 1089–1115.

Rodríguez-Serrano M, Pazmiño DM, Sparkes I, Rochetti A, Hawes C, Romero-Puertas MC, Sandalio LM. 2014. 2,4-Dichlorophenoxyacetic acid promotes *S*-nitrosylation and oxidation of actin affecting cytoskeleton and peroxisomal dynamics. Journal of Experimental Botany **65**, 4783–4793.

Rodríguez-Serrano M, Romero-Puertas MC, Sparkes I, Hawes C, del Río LA, Sandalio LM. 2009. Peroxisome dynamics in Arabidopsis plants under

oxidative stress induced by cadmium. Free Radical Biology and Medicine **47**, 1632–1639.

Romero-Puertas MC, McCarthy I, Gómez M, Sandalio LM, Corpas FJ, del Río LA, Palma JM. 2004a. Reactive oxygen species-mediated enzymatic systems involved in the oxidative action of 2,4-dichlorophenoxyacetic acid. Plant, Cell and Environment **27**, 1135–1148.

Romero-Puertas MC, Corpas FJ, Sandalio LM, Leterrier M, Rodríguez-Serrano M, del Río LA, Palma JM. 2004b. Glutathione reductase from pea leaves: Response to abiotic stress and characterization of the peroxisomal isozyme **170**, 43-52.

Rosenwasser S, Fluhr R, Joshi JR, Leviatan N, Sela N, Hetzroni A, Friedman H. 2013. ROSMETER: a bioinformatic tool for the identification of transcriptomic imprints related to reactive oxygen species type and origin provides new insights into stress responses. Plant Physiology **163**, 1071–1083.

Sandalio LM, Peláez-Vico MA, Molina-Moya E, Romero-Puertas MC. 2021. Peroxisomes as redox-signaling nodes in intracellular communication and stress responses. Plant Physiol, kiab060.

Sandalio LM, Rodríguez-Serrano M, Romero-Puertas MC. 2016. Leaf epinasty and auxin: a biochemical and molecular overview. Plant Science **253**, 187–193.

Sandalio LM, Romero-Puertas MC. 2015. Peroxisomes sense and respond to environmental cues by regulating ROS and RNS signalling networks. Annals of Botany **116**, 475–485.

Schilmiller AL, Koo AJK, Howe GA. 2007. Functional diversification of acyl-coenzyme A oxidases in jasmonic acid biosynthesis and action. Plant Physiology **143**, 812–824.

Smyth GK, Speed T. 2003. Normalization of cDNA microarray data. Methods **31**, 265–273.

Teixeira MC, Duque P, Sá-Correia I. 2007. Environmental genomics: mechanistic insights into toxicity of and resistance to the herbicide 2,4-D. Trends in Biotechnology **25**, 363–370.

Terrón-Camero LC, Peláez-Vico MA, del-Val C, Sandalio LM, Romero-Puertas MC. 2019. Role of nitric oxide in plant responses to heavy metal stress: exogenous application versus endogenous production. Journal of Experimental Botany **70,** 4477–4488.

Terrón-Camero LC, Rodríguez-Serrano M, Sandalio LM, Romero-Puertas MC. 2020. Nitric oxide is essential for cadmium-induced peroxule formation and peroxisome proliferation. Plant Cell and Environment **43**, 2492–2507.

Ueda J, Miyamoto K, Góraj-Koniarska J, Saniewski M. 2018. Petiole bending in detached leaves of *Bryophyllum calycinum*: relevance to polar auxin transport in petioles. Acta Biologica Cracoviensia Series Botanica **60**, 25–33.

Vanderauwera S, Zimmermann P, Rombauts S, Vandenabeele S, Langebartels C, Gruissem W, Inzé D, Van Breusegem F. 2005. Genome-wide analysis of hydrogen peroxide-regulated gene expression in Arabidopsis reveals a high light-induced transcriptional cluster involved in anthocyanin biosynthesis. Plant Physiology **139**, 806–821.

Zuanazzi NR, Ghisi NC, Oliveira EC. 2020. Analysis of global trends and gaps for studies about 2,4-D herbicide toxicity: a scientometric review. Chemosphere **241**, 125016.

Table 1: ACX1-dependent genes related to auxin metabolism and signalling. Transcripts regulated in WT but not in *acx1-2* mutants after 2,4-D treatment at 1 and 72 hpt, related to auxin metabolism and signalling.

	Transcript ID	mutant	GO clasification	Target Description
1h-up	At1g04100		[GO:0009733] response to auxin stimulus	IAA10__indoleacetic acid-induced protein 10
	At1g75500		[GO:0090355] positive regulation of auxin metabolic process	WAT1__Walls Are Thin 1
	At2g34650		[GO:0009733] response to auxin stimulus	ABR_PID__Protein kinase superfamily protein
	At3g16500		[GO:0009733] response to auxin stimulus	IAA26_PAP1__phytochrome-associated protein 1
	At3g28910	SALK_027644C	[GO:0009733] response to auxin stimulus	ATMYB30_MYB30__myb domain protein 30
	At3g63420		[GO:0010541] acropetal auxin transport	AGG1_ATAGG1_GG1__Ggamma-subunit 1
	At4g23570	SALK_122139C	[GO:0071365] cellular response to auxin stimulus	SGT1A__phosphatase-related
	At4g36800		[GO:0009733] response to auxin stimulus	RCE1__RUB1 conjugating enzyme 1
	At5g35735		[GO:0031348] negative regulation of defense response	Auxin-responsive family protein
	At5g35570		[17.2.2] hormone metabolism.auxin.signal transduction	O-fucosyltransferase family protein
	At1g68370	SALK_031635C	[17.2.2] hormone metabolism.auxin.signal transduction	ARG1__Chaperone DnaJ-domain superfamily protein
	At1g14000		response to auxin stimulus GO:0009733	VIK__VH1-interacting kinase
	At5g45710	SALK_138256C	response to auxin stimulus	AT-HSFA4C_HSFA4C_RHA1__winged-helix DNA-binding TF family protein
	At5g54490		response to auxin stimulus	PBP1__pinoid-binding protein 1
1h-down	At1g12820	SALK_068787C	[GO:0000394] RNA splicing, via endonucleolytic cleavage and ligation	AFB3__auxin signaling F-box 3
	At1g28010	SALK_026876C	[GO:0010315] auxin efflux	ABCB14_ATABCB14_MDR12_PGP14__P-glycoprotein 14
	At1g28010		[GO:0010540] basipetal auxin transport	ABCB14_ATABCB14_MDR12_PGP14__P-glycoprotein 14
	At1g28440	SALK_141756C	[GO:0009926] auxin polar transport	HSL1__HAESA-like 1
	At2g21210	SALK_050249C	[GO:0015995] chlorophyll biosynthetic process	SAUR-like auxin-responsive protein family
	At2g22670		[GO:0009733] response to auxin stimulus	IAA8__indoleacetic acid-induced protein 8
	At2g33860	SALK_005658C	[GO:0009855] determination of bilateral symmetry	ARF3_ETT__TF B3 family protein / auxin-responsive factor AUX/IAA-related
	At2g47750		[GO:0009733] response to auxin stimulus	GH3.9__putative indole-3-acetic acid-amido synthetase GH3.9
	At3g02260	SALK_105495C	[GO:0009826] unidimensional cell growth	ASA1_BIG_CRM1_DOC1_LPR1_TIR3_UMB1__auxin transport protein (BIG)
	At3g59060		[GO:0010928] regulation of auxin mediated signaling pathway	PIF5_PIL6__phytochrome interacting factor 3-like 6
	At3g62980	SALK_151603C	[GO:0009734] auxin mediated signaling pathway	AtTIR1_TIR1__F-box/RNI-like superfamily protein
	At4g25960		[GO:0010540] basipetal auxin transport	ABCB2_PGP2__P-glycoprotein 2
	At5g48900		[GO:0009926] auxin polar transport	Pectin lyase-like superfamily protein
	At5g49980		[GO:0007165] signal transduction	AFB5__auxin F-box protein 5
	At5g53590		[GO:0009733] response to auxin stimulus	SAUR-like auxin-responsive protein family
	At5g55910		[GO:0010540] basipetal auxin transport	D6PK__D6 protein kinase
	At1g60690		[17.2.3] hormone metab aux.induced-regulated-responsive-activated	NAD(P)-linked oxidoreductase superfamily protein
	At5g53588		hormone metabolism.auxin.signal transduction	CPuORF50_conserved peptide upstream open reading frame 50 SAUR-like aux-responsive protein fam
	At4g37260		[GO:0009733] response to auxin stimulus	ATMYB73_MYB73__myb domain protein 73
	At2g46830		[GO:0009733] response to auxin stimulus	AtCCA1_CCA1__circadian clock associated 1
	At2g37630		[GO:0009733] response to auxin stimulus	AS1_ATMYB91_ATPHAN_MYB91__myb-like HTH transcriptional regulator family protein

Table 1 (cont.): ACX1-dependent genes related to auxin metabolism and signalling

	Transcript ID	mutant	GO clasification	Target Description
72h-up	At1g80680	SALK_135920C	[GO:0009870] defense response signaling pathway	MOS3_NUP96_PRE_SAR3__SUPPRESSOR OF AUXIN RESISTANCE 3
	At5g65940	SALK_102725C	[GO:0009733] response to auxin stimulus	CHY1__beta-hydroxyisobutyryl-CoA hydrolase 1
	At4g16420		[GO:0009733] response to auxin stimulus	ADA2B_PRZ1__homolog of yeast ADA2 2B
	At2g26740		[GO:0009733] response to auxin stimulus	ATSEH_SEH__soluble epoxide hydrolase
	At3g09980		[GO:0009733] response to auxin stimulus	Family of unknown function (DUF662)
	At4g34710		[GO:0009733] response to auxin stimulus	ADC2_ATADC2_SPE2__arginine decarboxylase 2
	At5g64890		[GO:0009733] response to auxin stimulus	PROPEP2__elicitor peptide 2 precursor
	At4g33940	SALK_142877C	[GO:0009733] response to auxin stimulus	RING/U-box superfamily protein
	At5g02840	SALK_137617C	[GO:0009733] response to auxin stimulus	LCL1__LHY/CCA1-like 1
	At1g80680		[GO:0032502] developmental process	MOS3_NUP96_PRE_SAR3__SUPPRESSOR OF AUXIN RESISTANCE 3
	At3g16640		[GO:0010252] auxin homeostasis	TCTP__translationally controlled tumor protein
	At1g80680		[GO:0031965] nuclear membrane	MOS3_NUP96_PRE_SAR3__SUPPRESSOR OF AUXIN RESISTANCE 3
	At3g59060		[GO:0010600] regulation of auxin biosynthetic process	PIF5_PIL6__phytochrome interacting factor 3-like 6
	At5g54140		[GO:0009850] auxin metabolic process	ILL3__IAA-leucine-resistant (ILR1)-like 3
	At1g28440	SALK_141756C	[GO:0009926] auxin polar transport	HSL1__HAESA-like 1
	At4g23570	SALK_122139C	[GO:0071365] cellular response to auxin stimulus	SGT1A__phosphatase-related
	At3g16640		[GO:0009734] auxin mediated signaling pathway	TCTP__translationally controlled tumor protein
	At3g59060		[GO:0010928] regulation of auxin mediated signaling pathway	PIF5_PIL6__phytochrome interacting factor 3-like 6
	At3g15450		hormone metabolism.auxin.synthesis-degradation	Aluminium induced protein with YGL and LRDR motifs
	At3g55730	SALK_148462C	[GO:0009733] response to auxin stimulus	AtMYB109_MYB109__myb domain protein 109
	At4g09460		[GO:0009733] response to auxin stimulus	AtMYB6_MYB6__myb domain protein 6
	At3g09600	SALK_016333C	[GO:0009733] response to auxin stimulus	LCL5_RVE8__Homeodomain-like superfamily protein
	At2g26740		[GO:0009733] response to auxin stimulus	ATSEH_SEH__soluble epoxide hydrolase alpha/beta-Hydrolases superfamily protein
72h-down	At2g21050		[GO:0006865] amino acid transport	LAX2__like AUXIN RESISTANT 2
	At2g22670		[GO:0009733] response to auxin stimulus	IAA8__indoleacetic acid-induced protein 8
	At2g26730		[GO:0009926] auxin polar transport	Leucine-rich repeat protein kinase family protein
	At2g34680	SALK_113677C	[GO:0009733] response to auxin stimulus	AIR9__Outer arm dynein light chain 1 protein
	At2g47750		[GO:0009733] response to auxin stimulus	GH3.9__putative indole-3-acetic acid-amido synthetase GH3.9
	At4g12410	SALK_152759C	[GO:0009733] response to auxin stimulus	SAUR-like auxin-responsive protein family
	At4g25960		[GO:0010540] basipetal auxin transport	ABCB2_PGP2__P-glycoprotein 2
	At5g48900		[GO:0009926] auxin polar transport	Pectin lyase-like superfamily protein
	At1g17350		auxin response	NADH:ubiquinone oxidoreductase intermediate-associated protein 30
	At1g14020		auxin response	O-fucosyltransferase family protein
	At1g60690		auxin response	NAD(P)-linked oxidoreductase superfamily protein
	At1g74430		[GO:0009733] response to auxin stimulus	ATMYB95_ATMYBCP66_MYB95__myb domain protein 95

Table 2: Enrichment analysis of AFB3 using the String database.. GO categories related to biological process (BP), molecular function (MF), cellular component (CC) and KEGG pathways obtained following enrichment analysis of AFB3 using the String database, when no more than 10 interactors were selected.

BP	#term ID	term description	observed gene count	strength	false discovery rate
	GO:0016567	protein ubiquitination	10	1.55	2.01E-13
	GO:0006511	ubiquitin-dependent protein catabolic process	9	1.65	5.33E-13
	GO:0009987	cellular process	11	0.41	0.00017
	GO:0048527	lateral root development	2	1.7	0.0036
	GO:0021700	developmental maturation	2	1.46	0.0097
	GO:0009734	auxin-activated signaling pathway	2	1.42	0.0112
MF	GO:0010011	auxin binding	2	2.79	0.00015
CC	GO:0019005	SCF ubiquitin ligase complex	10	2.6	3.40E-24
	GO:0005634	nucleus	10	0.77	3.44E-07
	GO:0043231	intracellular membrane-bounded organelle	11	0.49	1.78E-05
	GO:0005623	cell	11	0.35	0.00032
KEGG pathways	ath04120	ubiquitin-mediated proteolysis	7	2.1	9.24E-14
	ath04141	protein processing in endoplasmic reticulum	7	1.93	7.20E-13

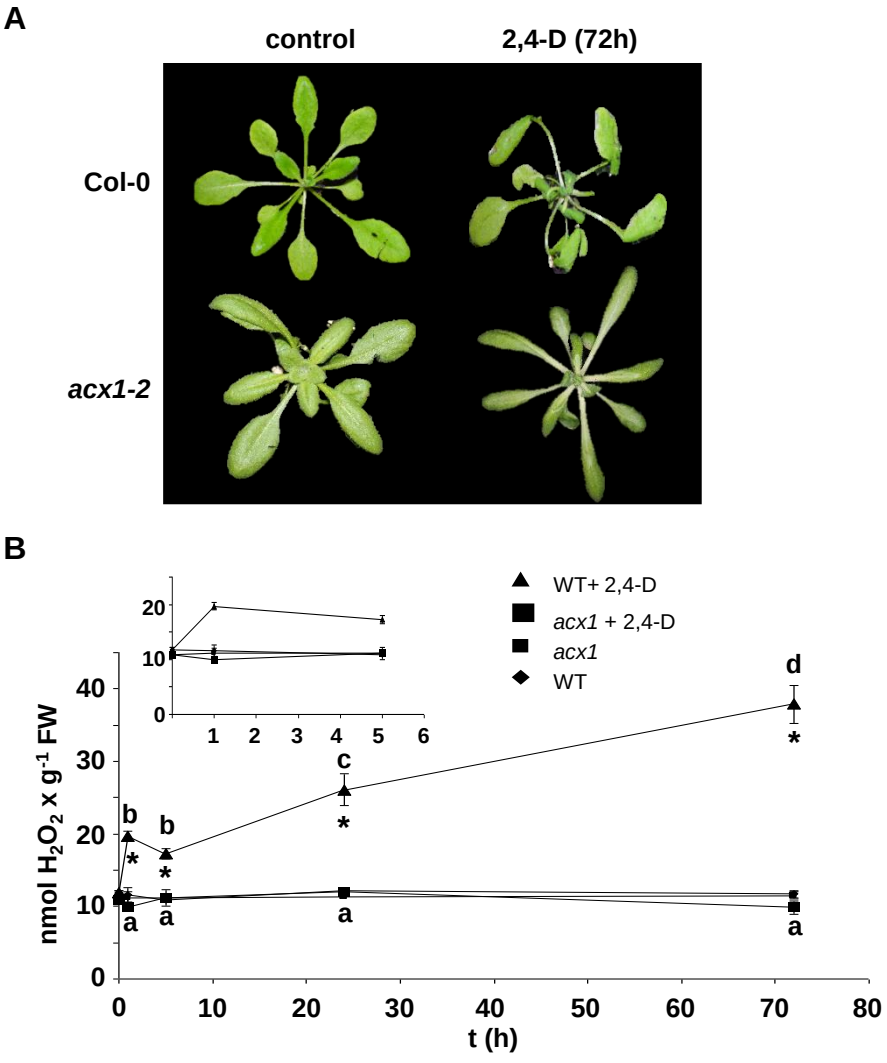

Figure 1. Effect of 2,4-D on plant phenotype and ROS production. A) WT and *acx1-2* plants were foliarly treated with 23 mM 2,4-D, whose phenotypic impact is shown (72 h). B) H_2O_2 content assayed by fluorimetry in acid extracts from WT and *acx1-2* leaves after plant spraying with 2,4-D (1 h-72 h). Values are means ± SE of at least three experiments with three independent extracts each. C) Confocal laser scanning microscopy (CLSM) imaging of H_2O_2 accumulation in cross-sections of Arabidopsis leaves using DCF-DA (Ex/Em: 485/530 nm). Images are maximal projections from several optical sections and are representative of at least 15 leaf sections from four different experiments. Different letters denote significant differences between 2,4-D treatment time points within the same genotype, obtained using Tukey multiple comparison tests (p-value < 0.05). The absence of letters indicates no significant differences. Asterisks denote significant differences between treated *acx1-2* and WT plants at each time point according to the Student's t-test (p-value < 0.05). The absence of an asterisk denotes no significant differences between *acx1-2* and WT plants under control conditions. x, xylem. Bar=300 µm

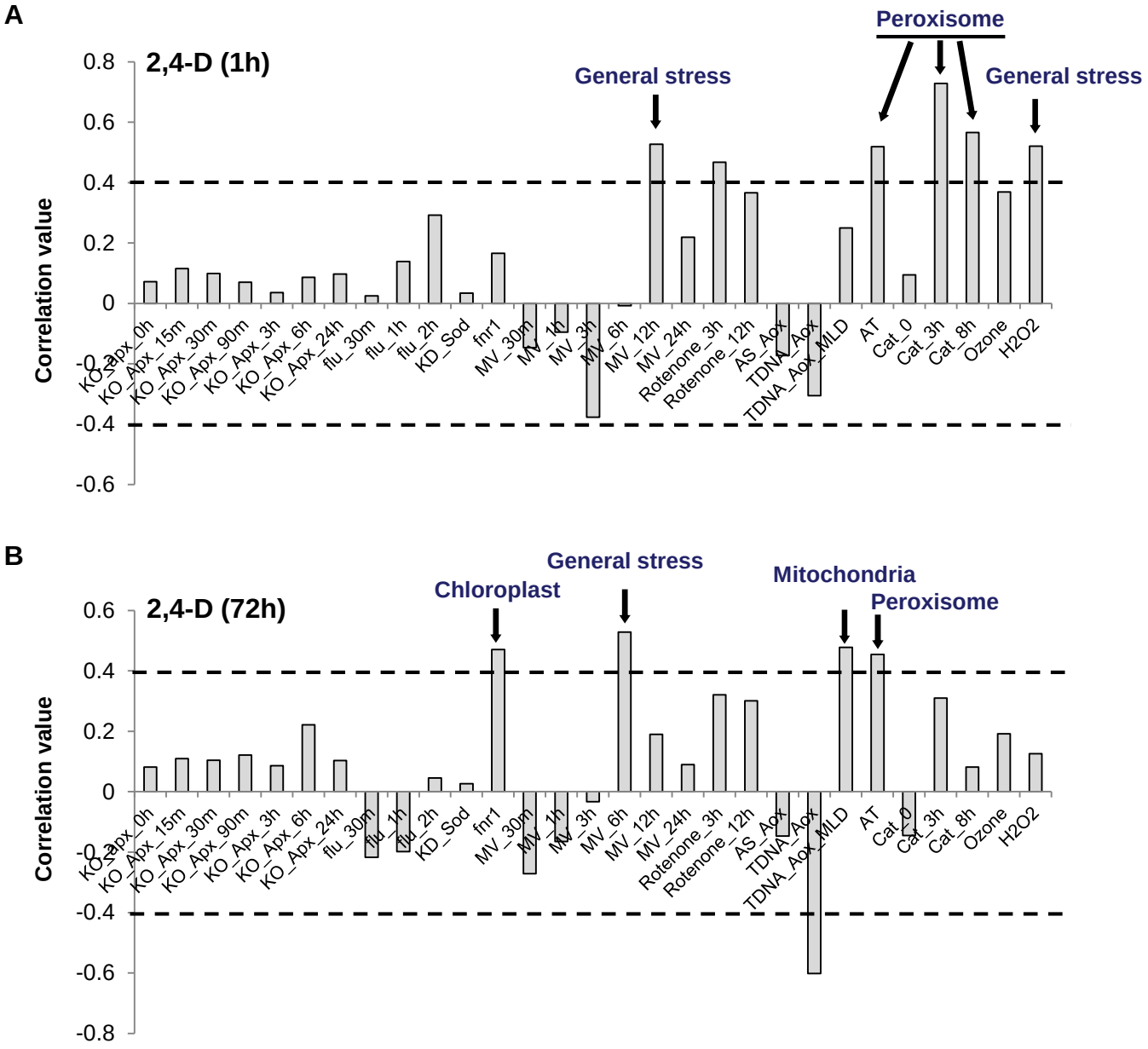

Figure 2. Analysis of 2,4-D transcriptome using the ROSMETER platform. Correlation values of changes in the transcriptome in WT Arabidopsis plants treated with 2,4-D for 1 h (A) and 72 h (B) generated by the ROSMETER platform. Correlation values (*y* axis, ordinate) were obtained as described by Rosenwasser et al. (2011, 2013) from the 2,4-D transcriptome and transcriptomes of the individual ROS-producing treatments compiled in the ROSMETER platform (*x* axis, abscissa) detailed in Suppl. Table S1 produced by Rosenwasser et al. (2013). Correlation value = 1 indicates complete correlation. Positive and negative data correspond to positive and negative correlation, respectively, between the transcriptomes. Correlation value = 0 indicates no correlation. Correlation values above 0,4 (discontinuous line) can be considered significant correlation values that provide biological insights (Rosenwasser *et al.,* 2013). Higher correlation values (arrows) at 1 h relate to peroxisomal stress (AT, aminotriazol treatment) cat_3h and cat_8h, *cat2-2* mutants under 3 and 8 h high light stress, respectively. Higher correlation values (arrows) at 72 h relate to peroxisomal stress (AT, aminotriazol treatment), general stress (methyl viologen, MV 6 h treatment), chloroplast stress (*fnr*1 mutants) and mitochondrial stress (*aox* mutants).

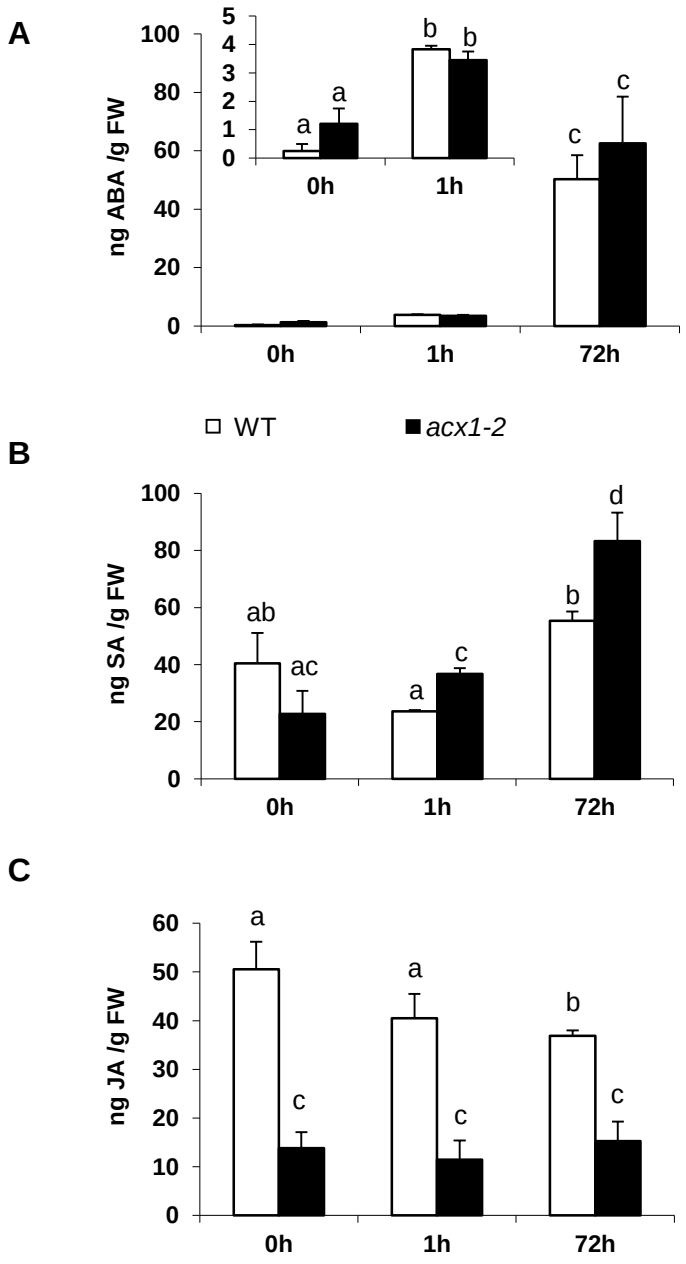

Figure 3. Effect of 2,4-D on plant hormone production. A) ABA, B) SA and C) JA production in WT and *acx1-2* plants after 2,4-D spraying at 1 h and 72 h. Amplification of the graph at 0 and 1 h treatment in A). Bars represent the mean ± SE of at least 4 replicates. Different letters denote significant differences between the different values obtained using Tukey multiple comparison tests (p-value < 0.05).

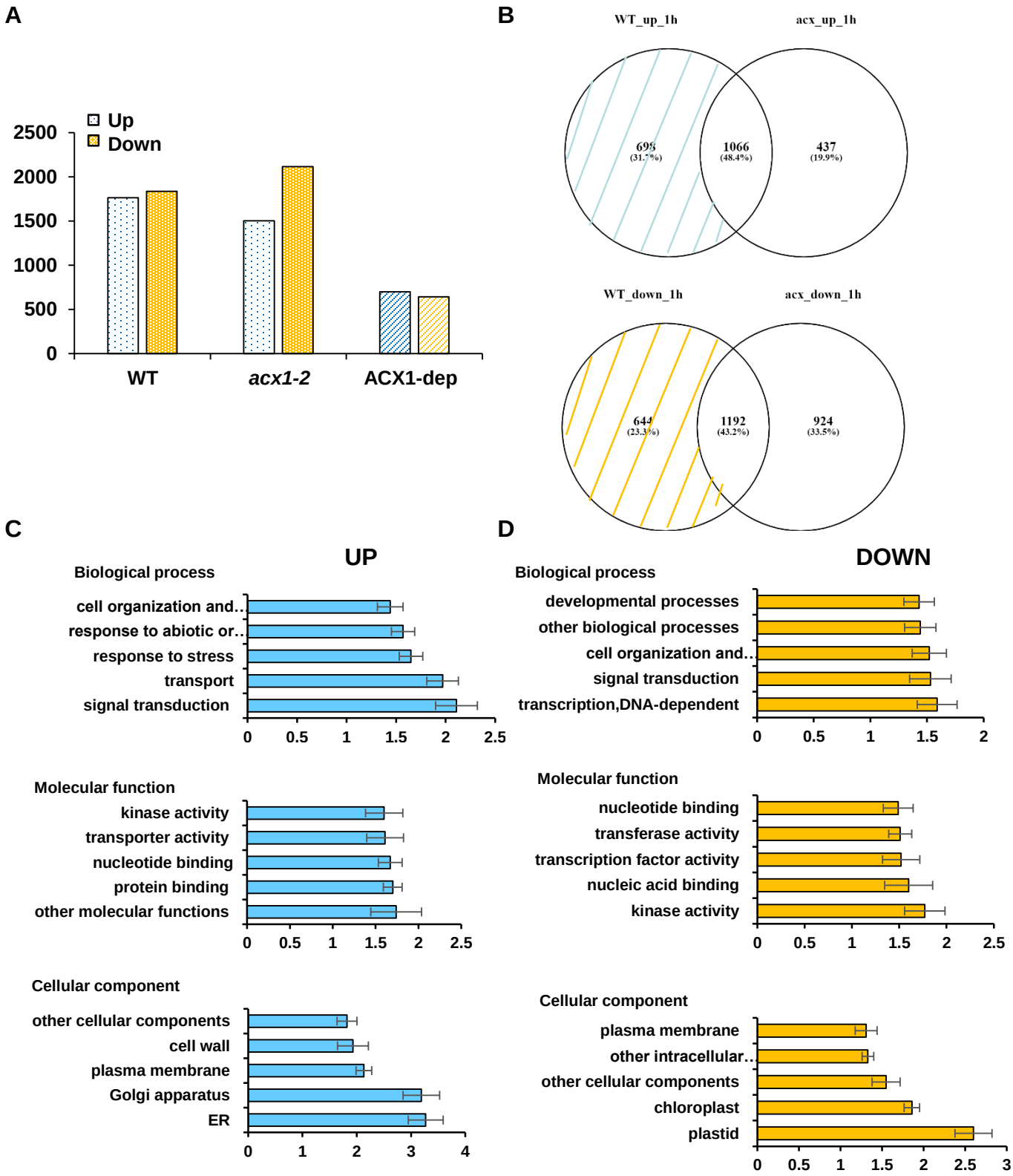

Figure 4. Changes in global transcript expression in the *acx1-2* mutant compared to wild type (WT) in response to short-term 2,4-D treatment. A) Number of up- and down-regulated genes in WT and *acx1-2* mutants after 1 h of 2,4-D spraying, and Venn diagrams B) showing the overlap between gene expression changes in WT and *acx1-2* mutants after 1 h of 2,4-D spraying; upregulated transcripts at the top and downregulated transcripts at the bottom. Transcript expression altered in the leaves of WT plants, but not of *acx1-2* mutants (ACX1-dependent) is marked by blue (up-regulated) and orange (down-regulated) coloured stripes. Five main categories after gene ontology (GO) enrichment of ACX1-dependent up- (C) and down- (D) regulated transcripts after 1h of 2,4-D spraying. Normed to frequency of class over all ID numbers on *x* axes.

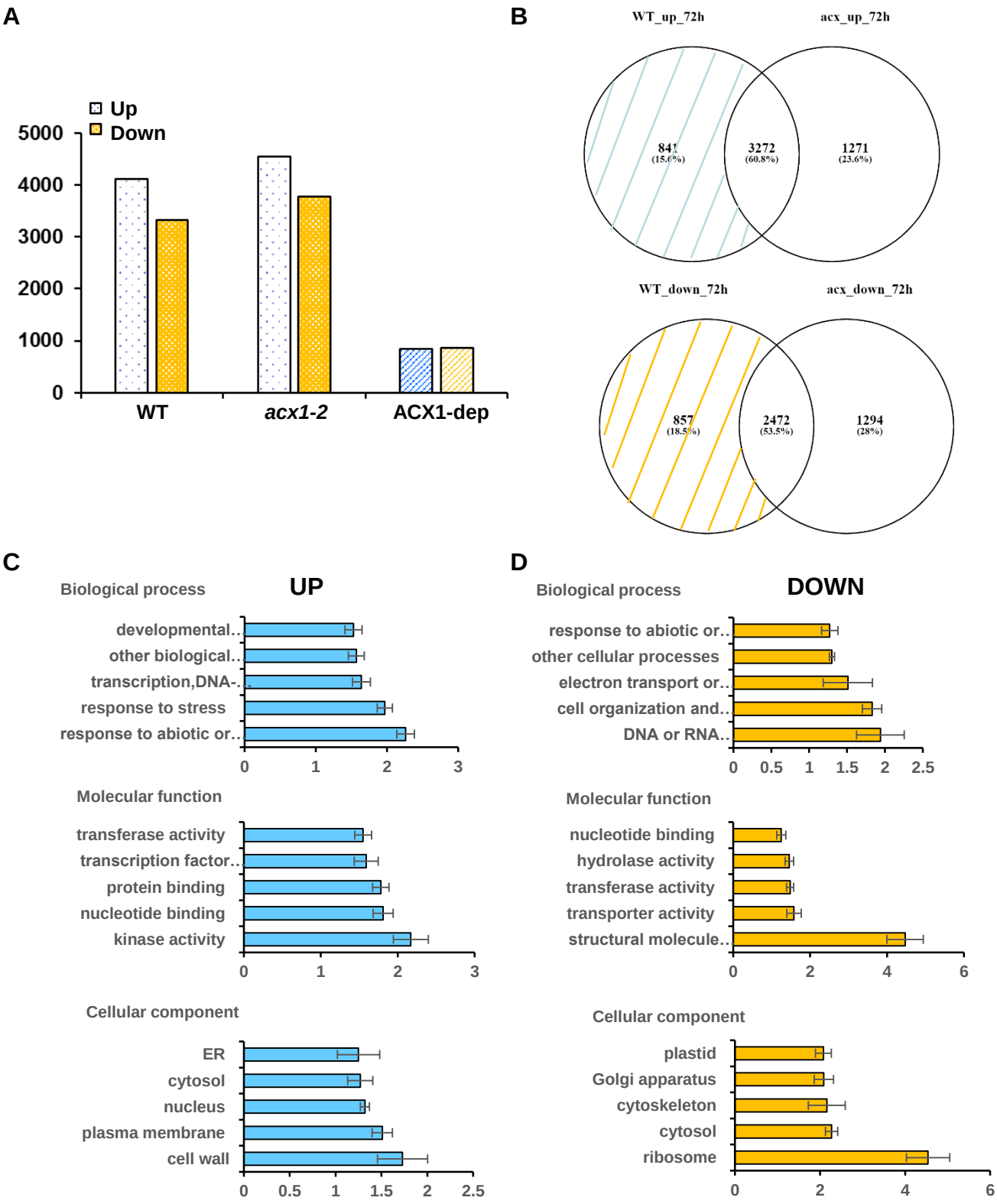

Figure 5. Changes in global transcript expression in the *acx1-2* mutant as compared to wild type (WT) in response to long-term 2,4-D treatment. A) Number of up- and down-regulated genes in WT and *acx1-2* mutants after 72 h of 2,4-D spraying, and Venn diagrams B) showing the overlap between gene expression changes in WT and *acx1-2* mutants after 72 h of 2,4-D spraying; up-regulated transcripts on top and down-regulated transcripts on bottom. Transcript expression altered in leaves of WT plants, but not in *acx1-2* mutants (ACX1-dependent), is marked by blue (up-regulated) and orange (down-regulated) coloured stripes. Five main categories after gene ontology (GO) enrichment of ACX1-dependent up- (C) and down- (D) regulated transcripts after 72 h of 2,4-D spraying. Normed to frequency of class over all ID numbers on *x* axes.

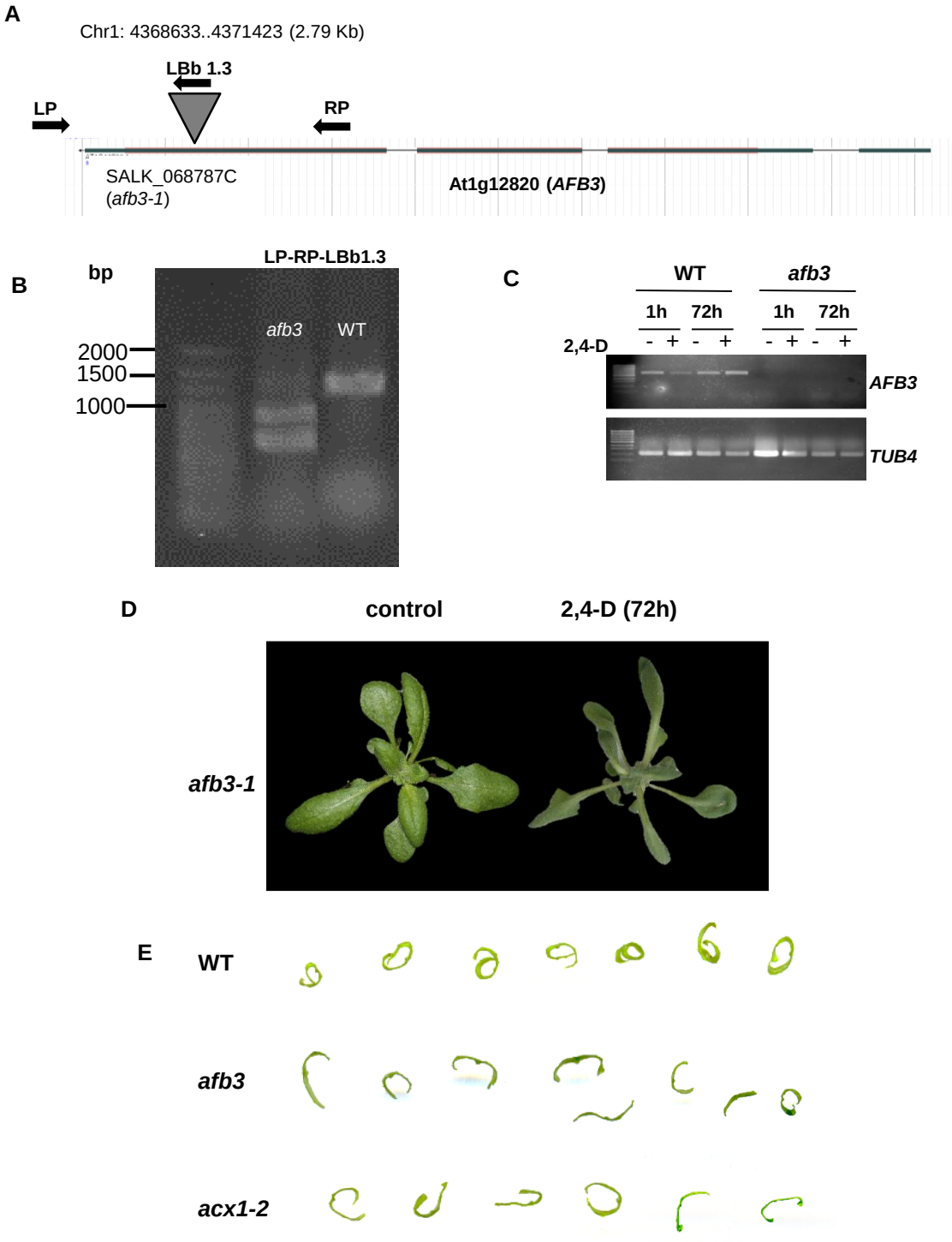

Figure 6: *afb3-1* genotyping and *AFB3* expression in plants treated with 2,4-D. A) Diagram showing the position of the T-DNA insertion and primers used (LP, RP and LBb1.3) for genotyping *afb3-1* mutant; B) PCR-based genotyping of WT and mutant plants. Ethidium bromide stained amplicons obtained when using LP, RP and LBb1.3 primers; C) Semi-quantitative RT-PCR analysis of *AFB3* transcript in WT and *afb3-1* leaves after 1 and 72 h of spraying with 2,4-D. No amplification of the transcript was observed following quantitative analysis of *afb3-1* mutants. D) WT, *afb3-1* and *acx1-2* plants were foliarly treated with 23 mM 2,4-D, whose effect on leaves phenotype is shown. Leaves were sliced after 72 h of 2,4-D spraying to better view epinasty.

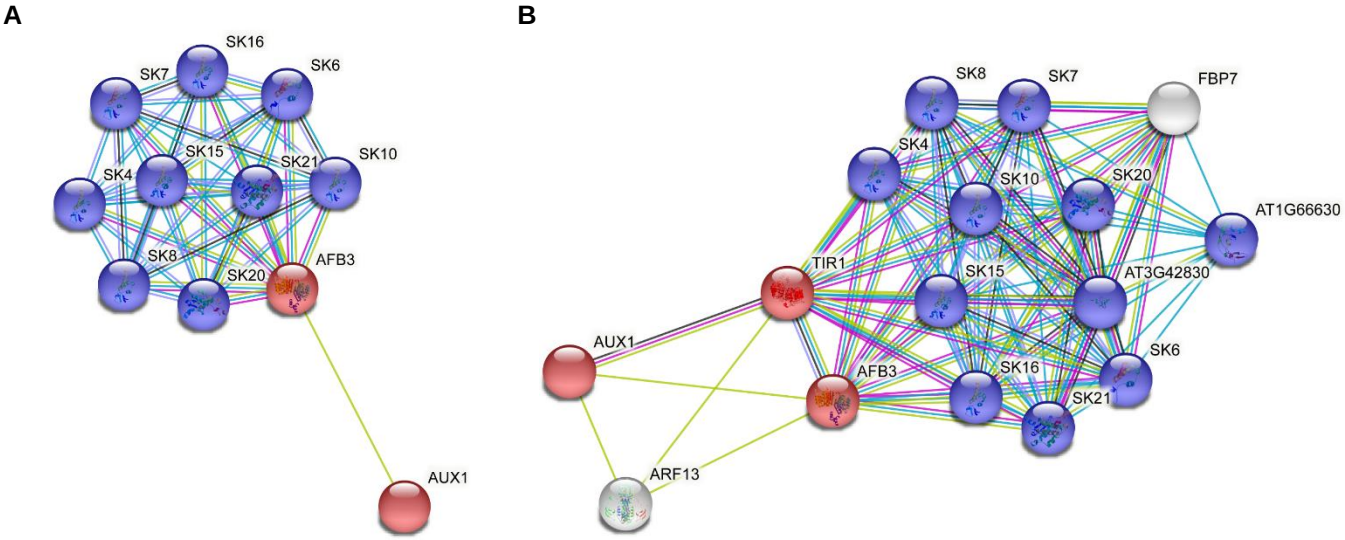

Figure 7: Predicted functional partners of AFB3. SKP1-like proteins involved in ubiquitination and subsequent proteasomal degradation of target proteins obtained using the stringDB tool (https://string-db.org/) following the selection of no more than 10 interactors (A) are the main partners of AFB3. Together with CUL1, RBX1 and AFB3, SKPs forms a SCF E3 ubiquitin ligase complex in which SKPs act as adapters linking AFB3 to CUL1. Similar results including five interactors in a second shell were obtained (B).

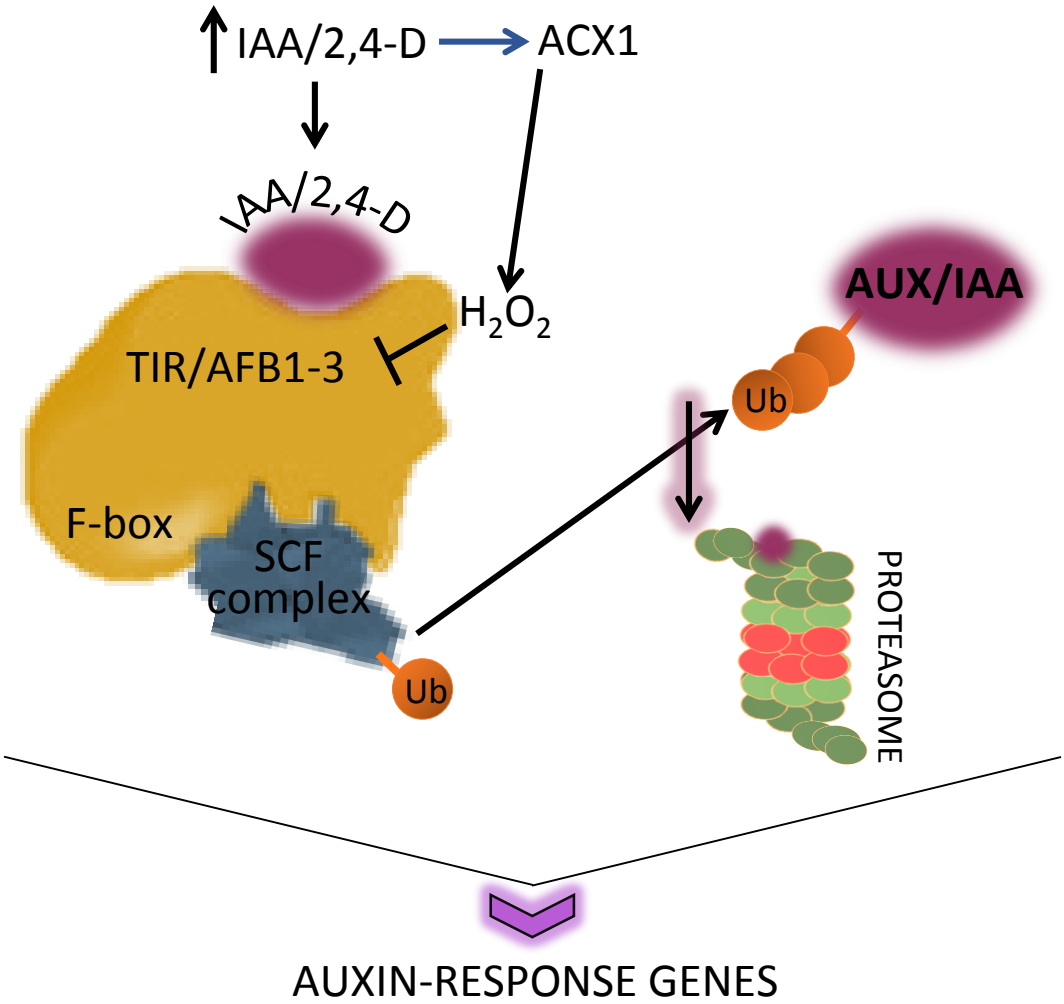

Figure 8: Scheme showing the possible mechanistic toxicity of 2,4-D in Arabidopsis plants. At high IAA levels, TIR1/AFB 1–3 increase the affinity for the AUX/IAA degron through direct IAA binding, resulting in AUX/IAA ubiquitination and further degradation, thus ensuring ARF de-repression and auxin-induced transcriptional changes. ACX1-dependent H_2O_2 is involved in the toxicity of the auxinic herbicide 2,4-D, regulating *AFB3* expression, thus enabling ubiquitination and degradation of AUX/IAA, leading to the modulation of auxin-responsive gene expression.

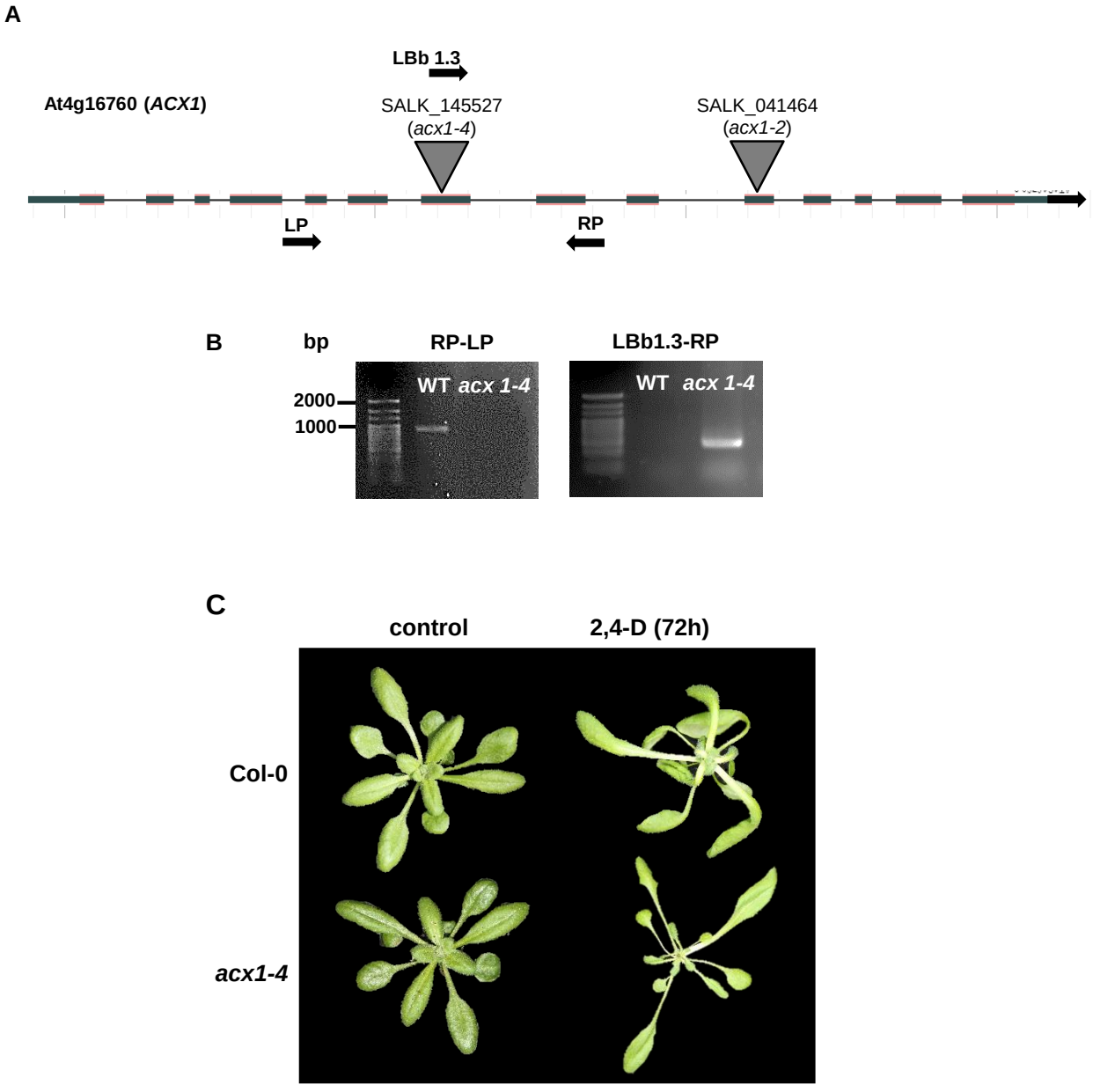

Suppl. Fig. S1: ***acx1-4* genotype and phenotype in plants treated with 2,4-D.** A) Diagram showing the position of the T-DNA insertion and primers used (LP, RP and LBb1.3) for genotyping *acx1-4* mutants. B) PCR-based genotyping of WT and mutant plants. Ethidium bromide-stained amplicons obtained when using LP, RP and LBb1.3 primers. C) WT and *acx1-4* plants were foliarly treated with 23 mM 2,4-D whose effect on the leaf phenotype is shown.

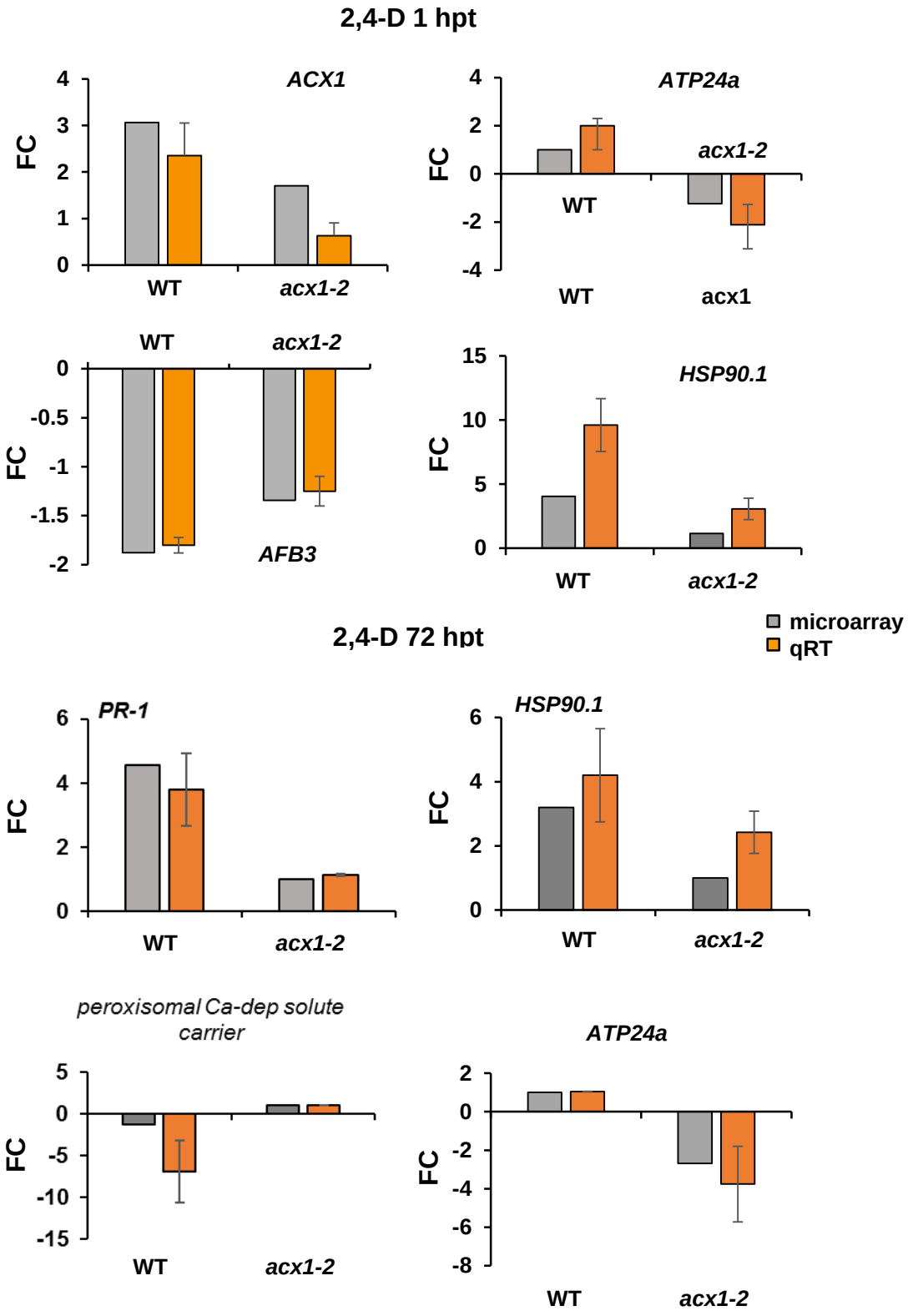

Suppl. Fig. S2: **Validation of microarray results.** Quantitative real-time PCR compared with fold change (FC) data obtained by microarray analyses of genes related to different categories. FCs using qRT-PCR were calculated as $2^{-\Delta\Delta Ct}$ (n= 3). Primers used are described in Supplemental Table S1. Each gene was normalized against *TUB4* expression.

A 2,4-D (1h)

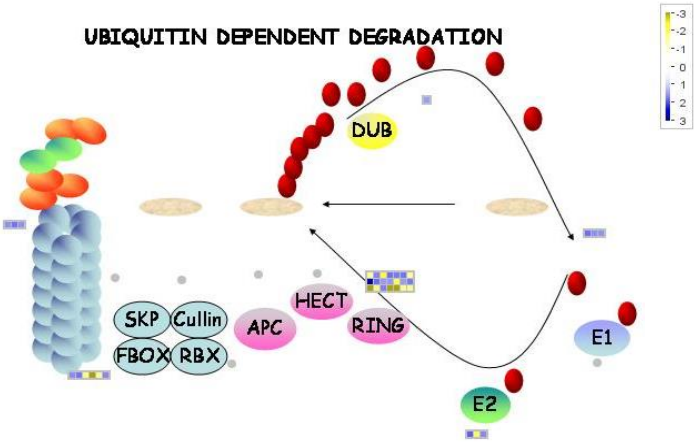

B 2,4-D (72h)

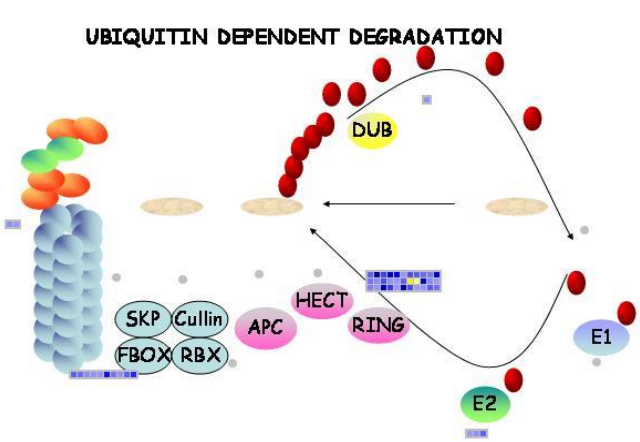

Suppl. Fig. S3: **Diagram of ACX1-dependent genes regulated by 2,4-D relating to ubiquitin-dependent degradation using MapMan.** A) After 1 h of 2,4-D treatment; B) after 72 h of 2,4-D treatment. At 72 hpt, protein degradation related to E3-RING and E3-SCF-FBOX ubiquitin categories (Suppl. Table S3), was significantly regulated.